Integrated Seismic and Well log Analysis for Improved Reservoir Characterization of Early Cretaceous Reservoir rock, DULJAN Block, Lower Indus Basin, Pakistan

BY

QAISER SULTAN

MPhil GEOPHYSICS

(2021-2023)

DEPARTMENT OF EARTH SCIENCE, QUAID-I-AZAM UNIVERSTY

ISLAMABAD, PAKISTAN

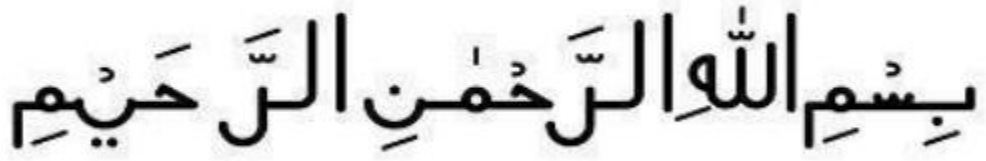

Start with the name of ALLAH, the most gracious and the most merciful. Free of defects, for whom is all praise, and he is the greatest. No one can do anything without his willingness.

CERTIFICATE

This dissertation submitted by **QAISER SULTAN S/O ATTA ULLAH** is accepted in its present form by the Department of Earth Sciences, Quaid-I-Azam University Islamabad as satisfying the requirement for award of MPhil Degree in Geophysics.

RECOMMENDED BY

Dr. Tahir Azeem
Assistant Professor /Supervisor _____

External Examiner
Dr. Muhammad Irfan Ahsan _____

Dr. Mumtaz M. Shah
Chairman _____

DEDICATION

I dedicate my work to Allah almighty, thanks Allah for the guidance, health and potential to complete this work. This work is also dedicated to my parents, brothers and sisters who supported me in all aspects of completing this work. And, thanks to my friends for their valuable advice, guidance, and support in doing this study.

ACKNOWLEDGEMENTS

Started with the name of Allah, The Most Gracious and the Most Merciful. Free of defects, for whom is all praise, and he is the greatest. No one can do nothing without his willingness, Holy Prophet Muhammad (PBUH) is the last messenger of Allah and whose life is perfect model for us. Thanks to Allah for the guidance, health and potential to complete this work.

Thanks to my respectable supervisor **Dr. Tahir Azeem** for his supervision, valuable advice, cooperation, and support in completing this dissertation. And, thanks to my seniors Yawar ameen and Umer Ghaffar for the guidance in the preparation of this thesis and the assistance in any way that I may have asked. I would like to express my appreciation to my whole family, especially my father, mother, brothers, and sister for their support and help without which I was unable to reach at this stage.

Thanks to faculty of the department for giving knowledge, support, cooperation, and guidance in doing this thesis. I sincerely thank all my friend especially (Farman Ullah, Nasar Ullah, Umer Farooq and Abdul Majeed) for their love, care, and support during the study.

Qaiser Sultan
M.Phil. Geophysics
(2021-2023)

ABSTRACT

Hydrocarbon exploration requires better understanding of substructure and facies of the area. The study area lies in the Lower Indus Basin. In the Lower Indus Basin, the sands of Lower Goru are producing reservoir. However, due to heterogenic nature it is difficult to delineate the reservoir sands based on single data set. In this dissertation, seismic and well log data sets are integrated through seismic inversion to characterize A, B, C and D intervals of Lower Goru Formation of DULJAN block, Lower Indus Basin, Pakistan. To understand the subsurface structure of DULJAN block, four horizons are picked on seismic sections with the help of synthetic seismogram and faults are also marked. The marked normal faults intersect the whole Cretaceous rocks. Overall, horst and graben structures were observed due to northeast-southwest extensional regime in the study area. Petrophysical analysis of DULJAN RE-ENTRY-01 and DULJAN EAST-01 indicates that the well DULJAN RE-ENTRY-01 has two zones of interests in C interval having thickness of 3 and 5 meters, effective porosity 10%, water saturation 39% and volume of shale 40%. The petrophysical results of DULJAN EAST-01 shows that it has four zones of interest with relatively small thicknesses of 3,4,5 and 6 meters in A interval having average effective porosity of 10%, average water saturation 16% and average volume of shale 33%. To analyze the lateral extent of hydrocarbon bearing zones, Band limited and sparse spike inversion was performed. Inversion results show low impedance values within the reservoir zone. Impedance and porosity values within the zone of interest are (9700 (m/s) *(g/cc)) and 0.11 v/v respectively. Overall, sparse spike inversion shows better results than band limited inversion with correlation of 0.97% and 0.88% respectively.

Table of Contents

List of Figures

List of Tables

Chapter No.1 Introduction

1.1 Introduction

Geophysical techniques have been used to study internal structures and to find economical and useful things for mankind present under the Earth. These techniques are sensitive to lateral and vertical changes in physical properties of the earths subsurface. Different techniques have been used that can distinguish these vertical and lateral variations and give them a number form. Only using seismic data, it is difficult to identify payable and non-payable zones (Ahmad, et al., 2021). Through seismic interpretation subsurface geological structures and lithology present in an area are delineated. Discontinuity on seismic sections does not always represent faults, it may be due to noise or complex stratigraphy. (Soleimani, 2016).

Seismic structural interpretation involves marking faults and horizons in the zones which are areas of interest for us. Faults are marked where they are intersecting the horizons to analyze whether faults are acting as traps for hydrocarbons or a path to escape.

Petrophysical analysis is used for improved reservoir characterization and to differentiate between zones where hydrocarbons are present or not (Yuedong & Hongwei, 2007). In Petrophysical analysis the following parameters are found to check reservoir properties; porosity, permeability, volume of shale and water/hydrocarbon saturation. Generally, in petrophysical analysis gamma ray log tells us about lithology, laterolog deep (LLD) and laterolog shallow logs (LLS) tells about fluid and density and porosity logs about fluid and porosity of the rocks. Facies analysis is also an important technique for improved reservoir characterization and finding the lithology of reservoir and through it estimating the effectiveness of reservoir.

Through seismic inversion physical properties of rocks and fluid are determined from seismic data (Krebs, et al., 2009). Seismic inversion is also an important technique for improved reservoir delineation. Acoustic impedance is the most important property in inversion, obtained from density and velocity product, which indicate zones of interests. Different inversion types can be used, on the basis, which type best determines subsurface geology and stratigraphy. So, seismic inversion is one of the most important techniques in exploring oil and gas.

1.2 Geographical location of study area

The DULJAN block is located about 42Km southwest of Sawan plant in Gambat block, Khairpur district, Sindh province, Pakistan. It is present to the lower side of Jacobabad high. It is situated in the Lower Indus Basin, with respectively latitude and longitudes at 26° 39′ 1.81″ N and 68° 45′ 57.38″ E shown in Figure 1.1 below.

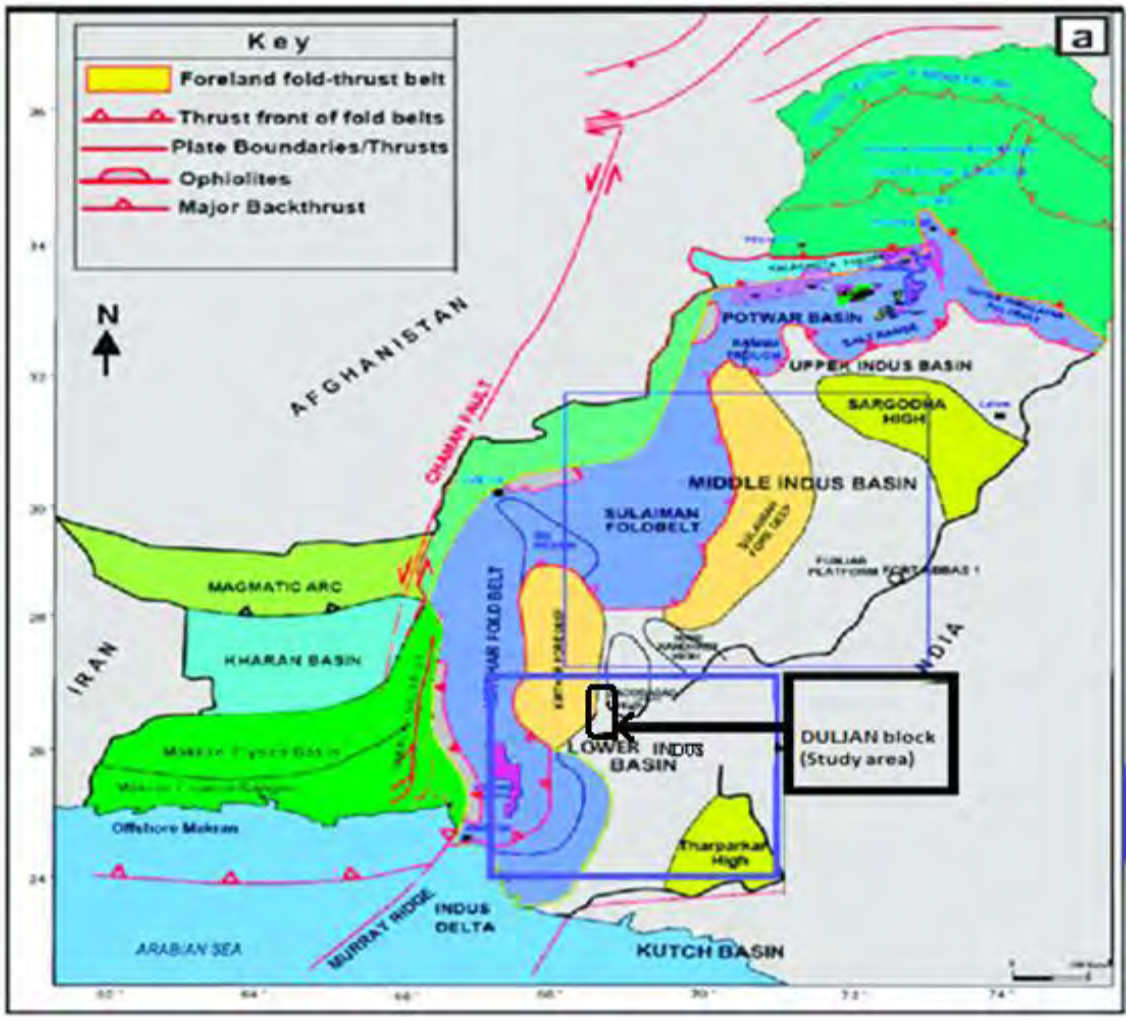

Figure 1.1: Geological map of Pakistan with geographical location of study area. (Anees et al., 2020)

1.3 Objectives

The main objectives of the study are as follows:

- Interpretation of 3D data to delineate the subsurface structural and stratigraphic traps for hydrocarbon accumulation.
- Petrophysical analysis to identify the zone of interest and quantification of reservoir parameters.
- Integration of different data sets through seismic inversion to identify the lateral extent of the reservoir in the study area.

1.4 Data Sets

Seismic and well data is used for improved reservoir characterization of DULJAN block. The formats for both data sets are mentioned below:

Seismic data (SEG-Y format)

Well log data (LAS file)

1.4.1 Seismic data

Table 1.1 contains the information of seismic dataset that is used in research purpose. These seismic inline and crossline combine to form a 3D seismic cube which is used for research purpose. In 3D seismic cube crossline number range is 271 to 485 and contains total 215 crosslines whereas inline number range is 321 to 534 and contain total 214 inlines.

Table 1.1: Seismic data used for research purpose.

Lines	**Start**	**End**	**Total number of Lines**
Crossline	271	485	215
In-Line	321	534	214

1.4.2 Base Map

Base map shows the location of inlines and crosslines on geographic coordinates at which seismic survey data have been acquired and the exact location of wells. The base map is shown in Figure 1.2 below.

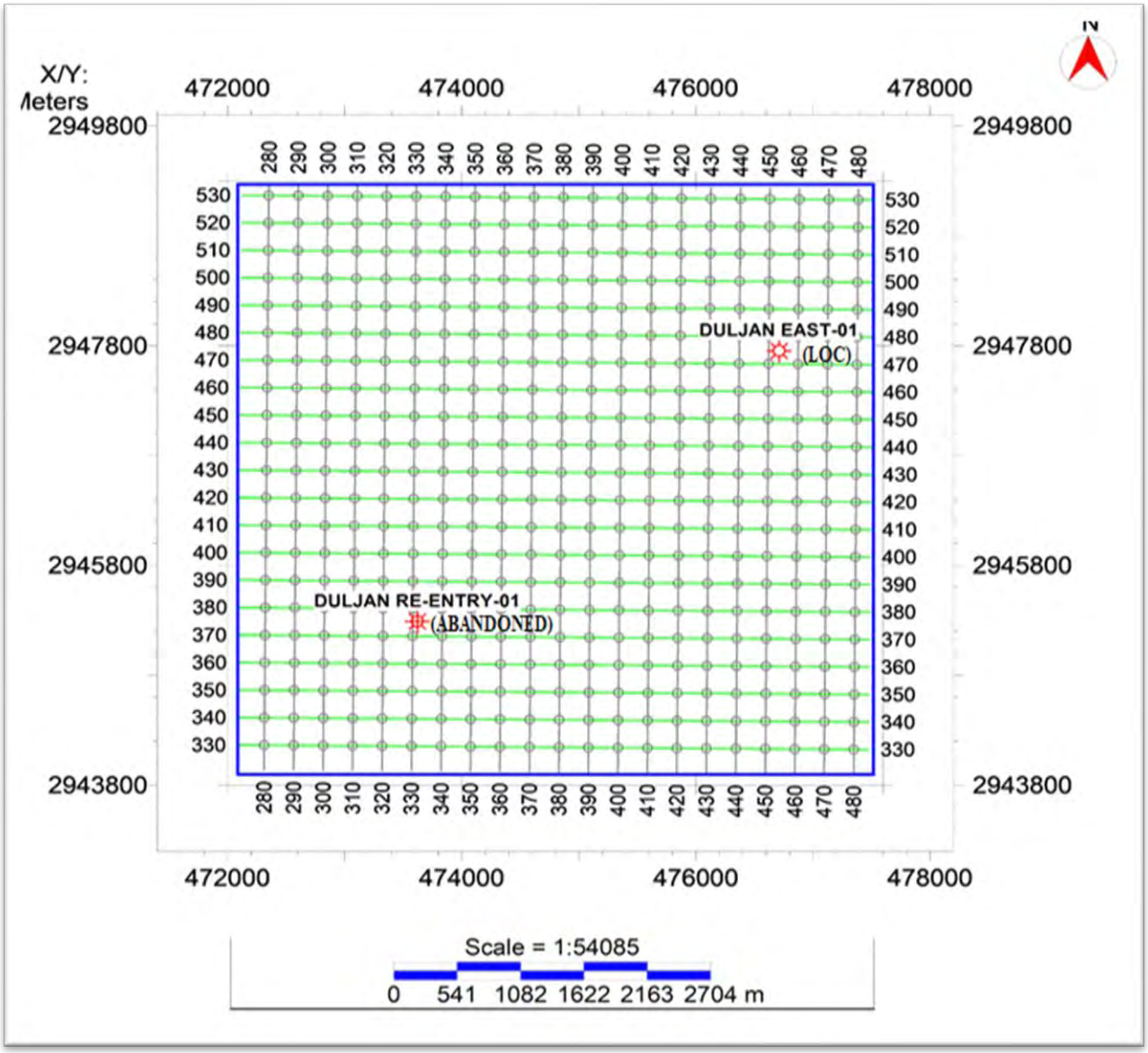

Figure 1.2: Basemap showing inlines, crosslines and well locations

1.4.3 Well Data

The information of well data used in research is shown in Tables 1.2 and 1.3 below.

Table 1.2: Shows well data of DULJAN EAST-01

Well Data			
Operator	OMV Pakistan	**Province**	Sindh
Type	Development	**Status**	LOC
Well Bore Name	DULJAN EAST-01	**Total Depth(m)**	3638.14
Longitude	68° 45′ 57.38″ E	**Latitude**	26° 39′ 1.81″ N
Elevation(m):	54	**Depth Reference**	KB

Well Tops			
Formations	**Formation Age**	**Top(m)**	**Thickness(m)**
ALLUVIUM-SIWALIKS	RECENT-MIOCENE	0	185
PIRKOH MEMBER	EOCENE	185	43
SIRKI MEMBER	EOCENE	228	57
HABIB RAHI MEMBER	EOCENE	285	215
LAKI	EOCENE	500	679
SUI MAIN LIMESTONE MEMBER	EOCENE	1179	178
RANIKOT	PALEOCENE	1357	967
UPPER GORU	LATE CRET/EARLY CRET	2324	292
LOWER GORU	EARLY CRETACEOUS	2616	523
D INTERVAL	EARLY CRETACEOUS	3139	24
C INTERVAL	EARLY CRETACEOUS	3163	135
B INTERVAL	EARLY CRETACEOUS	3298	180
A INTERVAL	EARLY CRETACEOUS	3478	74
SEMBAR	EARLY CRETACEOUS	3552	73

Table 1.3: Shows well data of DULJAN RE-ENTRY-01

Well Data			
Operator	OMV Pakistan	**Province**	Sindh
Type	Exploratory	**Status**	Abandoned
Well Bore Name	DULJAN RE-ENTRY-01	**Total Depth(m)**	3945.87
Longitude	68° 44′ 5.9″ E	**Latitude**	26° 37′ 41.5″ N
Elevation(m):	60	**Depth Reference**	KB

Well Tops			
Formations	**Formation Age**	**Top(m)**	**Thickness(m)**
ALLUVIUM-SIWALIKS	MIOCENE-PLEISTOCENEPLIOCENE	0	212
PIRKOH MEMBER	EOCENE	212	51
SIRKI MEMBER	EOCENE	263	39
HABIB RAHI MEMBER	EOCENE	302	199
GHAZIJ MEMBER	EOCENE	501	696
SUI MAIN LIMESTONE MEMBER	EOCENE	1197	184
RANIKOT	PALEOCENE	1381	929
UPPER GORU	LATE CRET/EARLY CRET	2310	278
LOWER GORU	EARLY CRETACEOUS	2589	585
D INTERVAL	EARLY CRETACEOUS	3174	19
C INTERVAL	EARLY CRETACEOUS	3193	143
B INTERVAL	EARLY CRETACEOUS	3337	175
A INTERVAL	EARLY CRETACEOUS	3513	20
SEMBAR	EARLY CRETACEOUS	3534	410

1.5 Methodology

To delineate and know the reservoir potential of Lower Goru intervals (A, B, C, D) in the study area, the methodology adapted in this research work is as follows:

- Identified the exact location of horizons on seismic section with the help of synthetic seismogram.
- Four horizons A, B, C and D intervals of Lower Goru reservoir Formation and the faults intersecting them are marked on seismic sections.
- Time and depth contour maps for marked horizons are generated to show the subsurface structural trend of intervals of Lower Goru Formation.
- Through Petrophysical analysis zones of interests are marked and reservoir parameters are quantified.
- Inversion is performed to identify the lateral extent of reservoir.
- Comparison of both inversions was done to know which type of inversion best discriminates against the subsurface geology.

1.6 Workflow of Dissertation

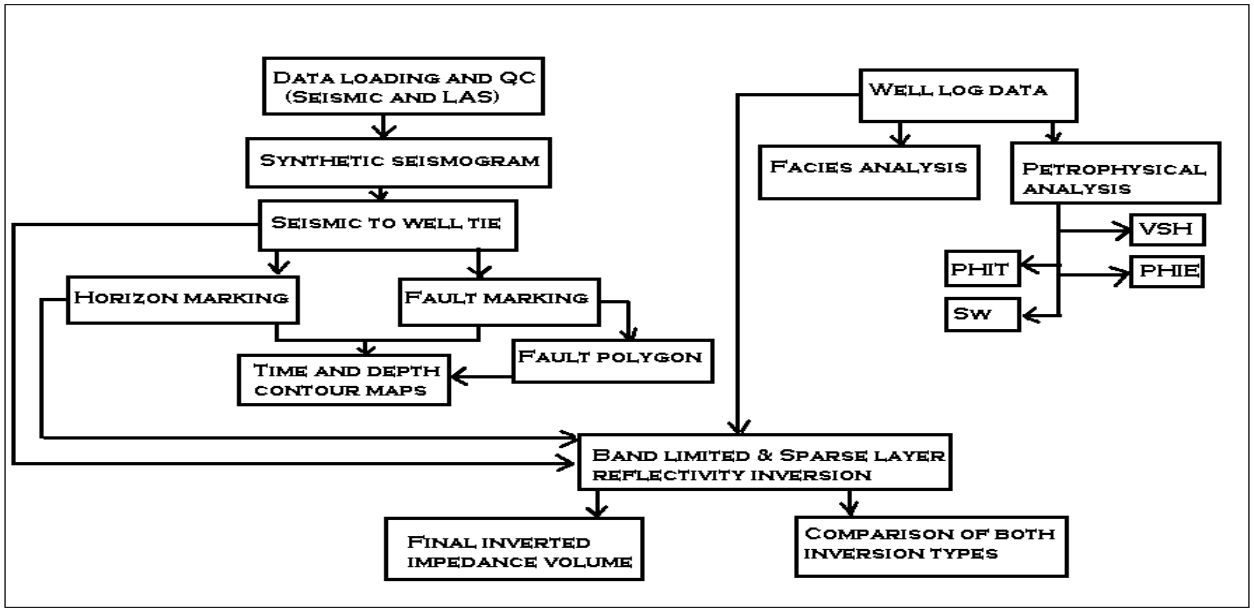

Figure 1.3: Workflow adopted for dissertation.

Chapter No.2 Tectonic and Geology

2.1 General geology and tectonic setting

Our area is DULJAN block lie in Khairpur area, Sindh province, Lower Indus Basin, Pakistan. It is bounded in the east by the Mari–Khandkot–Jaisalmer High, in west by the Kirthar Foldbelt and Foredeep (Fig.2.1) and the Jacobabad High separates the central and lower Indus Basins (Kemal et al., 1992) and the upper and central Indus basins are separated by Sargodha high. The lithostratigraphic nomenclature of Indus basin was formed by the geological survey of India. (Blanford, 1879). This nomenclature was developed from outcrop section measurements and hydrocarbon exploration data of the basin (Kemal et al., 1992).

Lower Indus Basin structures and geology is mainly controlled by tectonic events of rifting of the Indian Plate from Gondwanaland in Jurassic or Early Cretaceous times which formed NE-SW to N-S rift systems. This caused uplifting and some NNW-striking normal faults in the region. Gentle folding is also observed in the region.

Large anticlines and domes structures are present in the kirthar and Karachi depressions some of which contain some small fields of gas. Sindh monocline (Indus platform) in eastern part of the basin also contains some faults and tilted blocks which form structural traps.

2.2 Indus Basin

The Indus Basin, a region of immense geological significance, is of particular interest to the energy sector due to its notable hydrocarbon potential. The hydrocarbon potential of the Indus Basin is a focal point of exploration and analysis, drawing attention to its geological significance. Investigations into this basin's sedimentary layers and structural composition are aimed at identifying hydrocarbon reserves.

Covering about 875,000 kms of the area, the great Indus basin covers mostly eastern Pakistan and western parts of India. Indus Basin is subdivided into three basins: Upper Indus Basin, Central Indus Basin, and Lower Indus Basin.

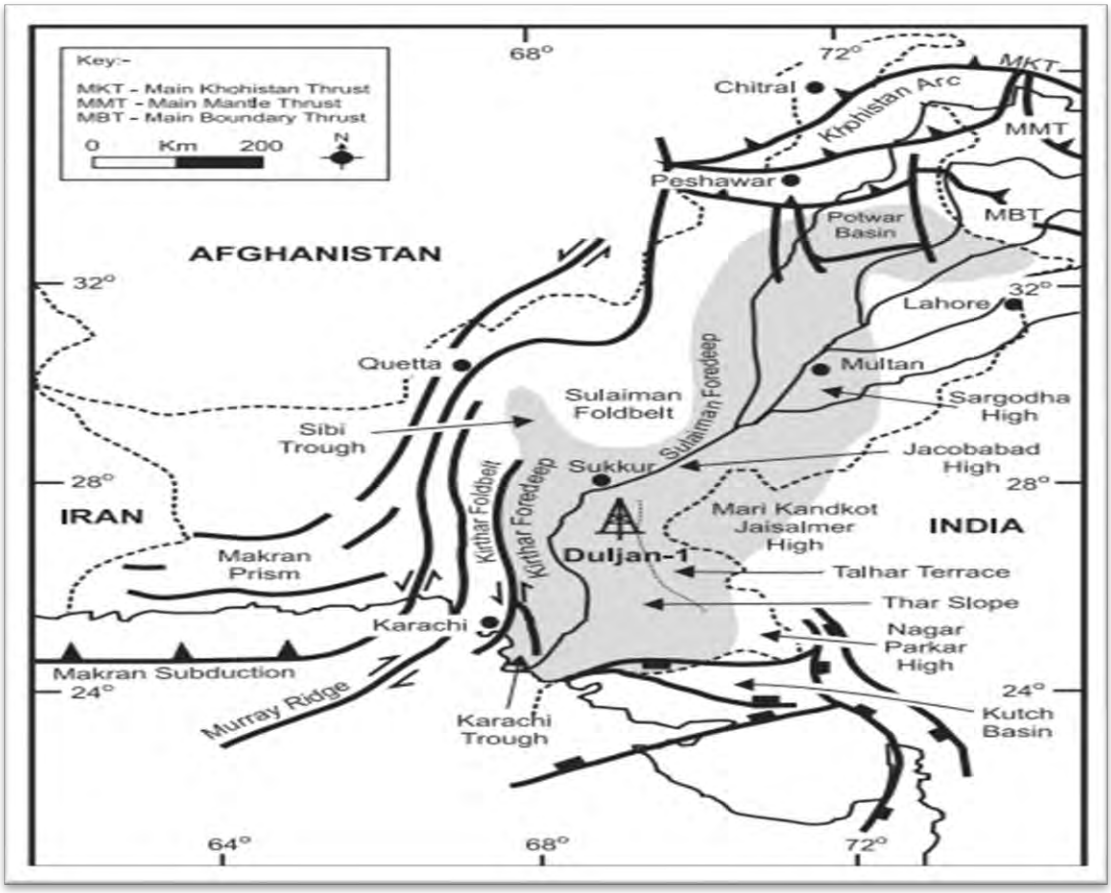

Figure 2.1: General geology of Indus Basin (Kemal et al., 1992)

2.2.1 Lower Indus Basin

It is bounded in north by the central Indus basin, in the southwest by the kirtharfold belt, in the northwest by Suleiman fold belt basin and in the east by mari–khandkot–jaisalmer high. Structural traps are found in Khairpur high region, Lower Indus Basin, Pakistan. (Ashraf et al., 2020). These faults are acting as a seal for hydrocarbon accumulation. Thick deposits of Marl and shale of upper Goru are main seals in the basin. The intra shales of Lower Goru are also acting as a seal in this area. (Kadri et al., 1995)

In the Lower Indus Basin massive sedimentation occurs in Triassic to the Quaternary ages (Raza et al., 1990). It is main source for production of oil and gas in Pakistan. Normal faulting is present in the Khairpur area. (Shuaib, 1981). Sembar formation is the main source in the Lower Indus Basin (Kadri, 1995).

2.3 Stratigraphy

The stratigraphy in the area ranges from infra-Cambrian to Recent clastic and carbonates. The stratigraphy of the area slightly changes from one area to another. Unconformities occur at the base of Permian and Tertiary. Tertiary and Jurassic sequence have direct contact with each other. The generalized stratigraphy of the DULJAN block, Khairpur, Sindh, Lower Indus Basin, Pakistan is shown below in Figure 2.2.

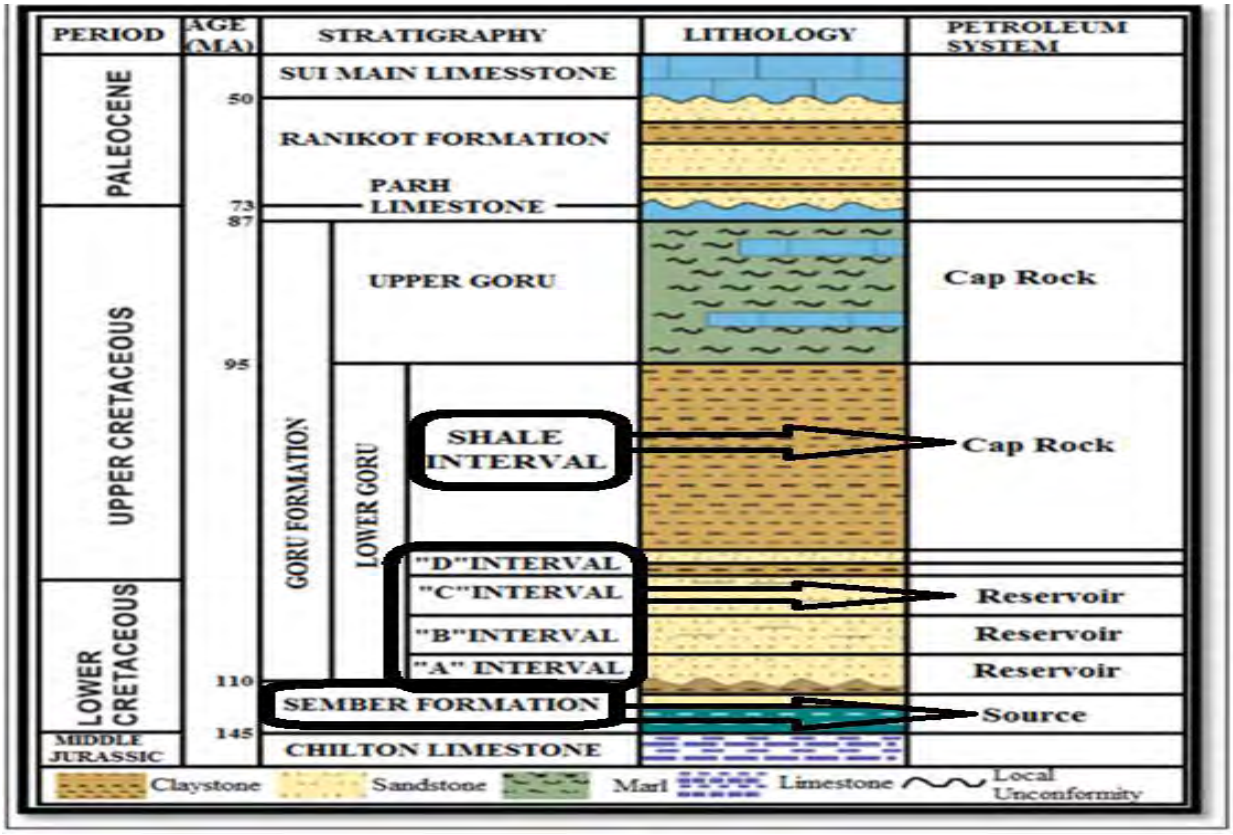

Figure 2.2: Generalized stratigraphy in the study area (Krois,1998)

2.3.1 Sembar Formation

Sembar is the lowermost unit of the Cretaceous sequence. It contains black shales interbedded with siltstone and limestone. With the overlying Goru Formation it has gradation contact and at some places an unconformity was also noted by Williams (1959). It is acting as source rock in the region.

2.3.2 Goru formation

Goru Formation contains interbedded shale, limestone, and siltstone. It ranges from Early cretaceous to Late cretaceous times. Sandstones in the formation are separated by shale. It was deposited in a marine environment. The presence of oysters and pelecypods also shows estuarine environment. (Raza et al., 1990).

It is further divided into:

- Lower Goru Formation
- Upper Goru Formation.

2.3.2.1 Lower Goru Formation

This Formation contains shale, shaly sand, sandy shale, sands, and marl. The Lower Goru Formation consists of four intervals A, B, C and D. A interval is present in the lower most part in this Formation and contains sandstone. Moving up comes B interval and this interval contains sandstone with shale beds. Above B comes the C interval, which also contains reservoir sands with interbedded shales. Intra formational shales of C interval serve as seal for the sandstones. Above all intervals is the D interval, consisting of sandstone with shale beds (Ahmad et al., 2004).

2.3.2.2 Upper Goru Formation

Upper Goru Formation is composed of thin bedded shales with some limestones. It is of the Late cretaceous age. It grades into the above Parh Limestone. It serves as seal for lower Goru reservoir Formation.

2.3.3 Park Limestone

It consists of thin bedded shales and marls. The limestone in this formation is platy with characteristic conchoidal fractures. It has gradational contact with the Goru Formation.

2.3.4 Ranikot Formation

Ranikot Formation is of Paleocene succession (Blandford et al., 1876). Ranikot has marine sequence of sandstones and shales with interbedded limestone (Khadro Formation).

2.4 Petroleum play

The Lower Goru Sands are the main reservoirs, Upper Goru and intra-Lower Goru shales are the main seals and Sembar Formation is source rock in the Indus Basin. The detailed description of source, reservoir and cap rock are given below:

2.4.1 Source

Lower Cretaceous Sembar formational shales are main source rock in the Basin due to richness of organic content and enough thermal maturity in it and have ability to generate gas. Due to the presence of type III kerogens, it produces gas.

2.4.2 Reservoir

Early Cretaceous to Eocene clastic and carbonates of Lower Goru Formation are main reservoir in the Basin. There are sand shale sequences in the reservoir from which sands are acting as reservoir. A, B, C and D, four intervals are present in the Lower goru Formation. Many producing wells are drilled from the Lower Goru reservoir.

2.4.3 Seal

Upper Goru Formation and shales within the lower Goru are acting as an excellent cap rock for lower Goru reservoir rock in the Basin.

2.4.4 Trapping mechanism

The tilted fault blocks and faulted gentle role-overs forms traps in the Basin. Stratigraphic traps may also be present. Extensional faulting in the area may also result in migration pathways for hydrocarbons along the fault planes.

Chapter No.3 Seismic data interpretation

3.1 Introduction

Seismic structural interpretation is the determination of subsurface geology and stratigraphy using seismic data. The main objective of seismic interpretation is to discover hydrocarbon traps in the subsurface. For seismic interpretation different software is used. Through these software grid contour maps are created which describe the structural trend of marked horizons on the base map. On grid contours maps the fault polygons can also been seen which indicate the orientation and length of faults (strike line of fault). Structure, sedimentary layering, stratigraphy, seismic velocities, and lithology all can be determined from good seismic data. (Dobrin and Savit, 1988)

Seismic reflection interpretation identifies the reflectors of interest and calculating their positions on seismic section through the sonic log (giving subsurface velocity) obtained from well data. After marking horizons and faults, contour maps for the horizons are generated that show fault strikes and the subsurface structural picture in time and depth domain. 214 inline and 215 crosslines were used to interpret subsurface structures of the DULJAN block, Khairpur, Sindh, Lower Indus Basin, Pakistan. For further refinement, well data of DULJAN EAST-01 and DULJAN RE-ENTRY-01 wells are used. The structural geometry has been studied by utilizing seismic data and well data of DULJAN block.

3.2 Workflow for seismic interpretation

Workflow adapted for seismic interpretation is shown below in Figure 3.1. In the workflow main steps are demonstrated, which are adapted for seismic interpretation. The main steps of workflow are loading well and seismic data, generation of synthetic seismogram, seismic to well tie, horizon marking, fault marking and then finally generation of time and depth contour maps.

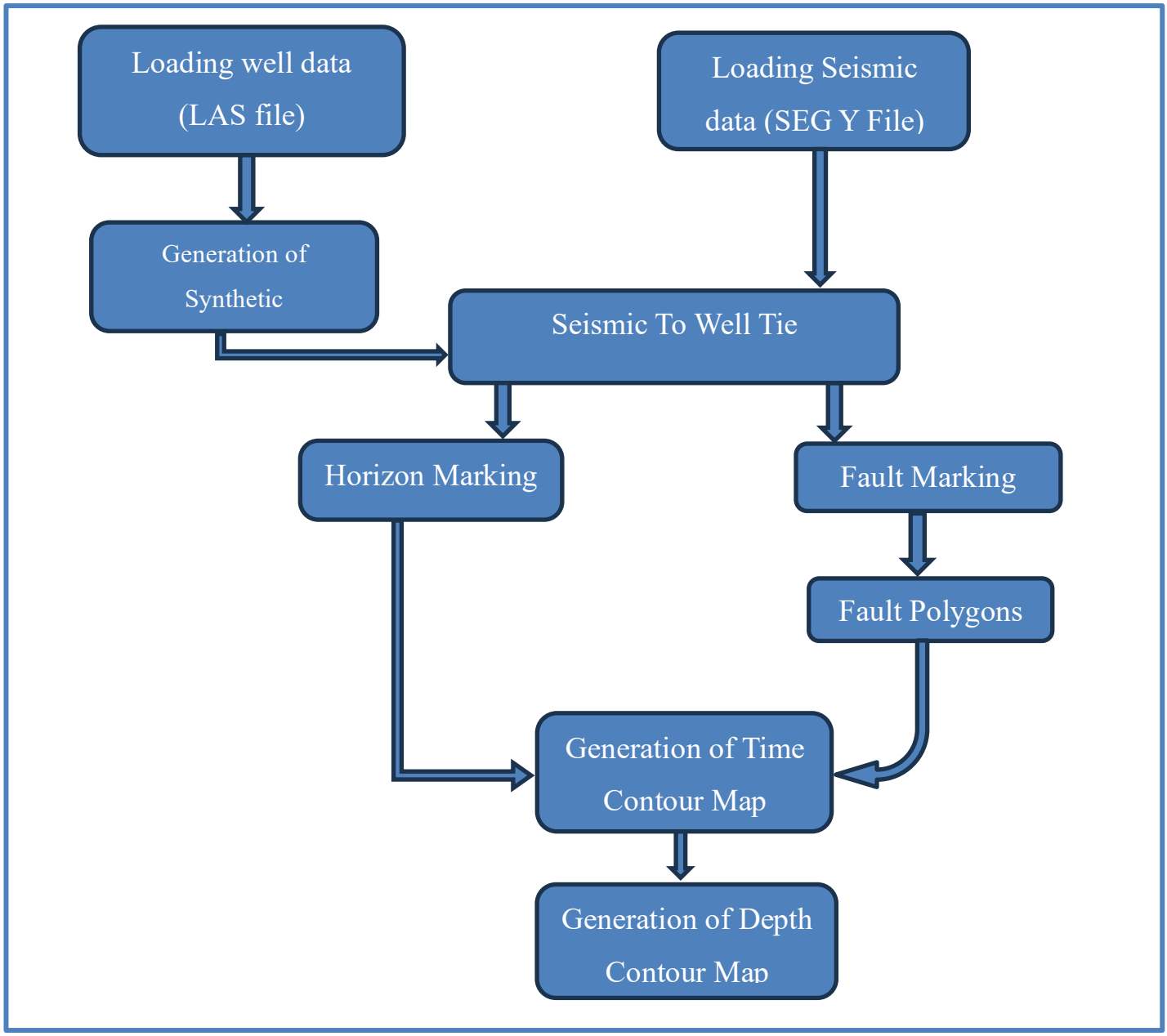

Figure 3.1: Workflow for Seismic Data Interpretation.

3.2.1 Loading data

Three types of data are loaded in software.

- Seismic data (SEG-Y format)
- Navigation data (X, Y)
- Well data (LAS file)

3.2.2 Generation of synthetic seismogram

Synthetic seismogram is generated by using sonic and density logs from well data. Time depth chart is used to know which Formation comes at which time on seismic section. Through the product of sonic and density logs impedance log is generated, from impedance log reflectivity series are generated and finally synthetic seismogram is generated by convolving wavelet (derived from seismic data) with reflectivity series. Synthetic seismogram generated from DULJAN RE-ENTRY-01 well is shown in Figure 3.2 below.

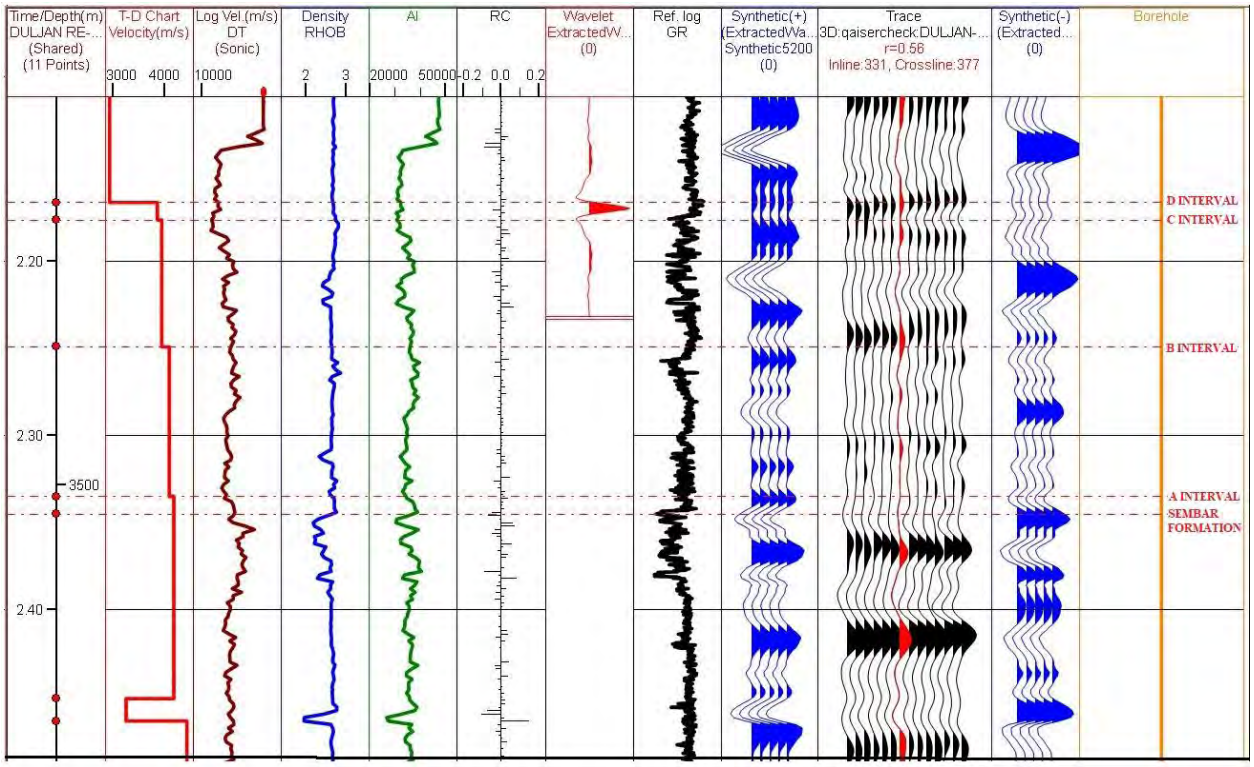

Figure 3.2: Synthetic Seismogram generated from DULJAN RE-ENTRY-01 well

3.2.3 Marking of seismic horizons and faults

To delineate the subsurface structure, four reflectors are marked on seismic sections based on the objective of the study i.e. for improved reservoir characterization. Four reflectors (A, B, C, D intervals) of Lower Goru Formation are marked and interpreted. Faults are also marked on given seismic inlines where the reflections are discontinuous. Four main normal faults are marked on

seismic lines. The pink line marks the A interval reflector, the cyan line marks the B interval reflector, the green line marks the C interval reflector, and the white line marks the D interval reflector. Whereas the yellow, blue, pink, and orange lines mark the corresponding F1, F2, F3 and F4 faults observed on the seismic lines. The seismic section shows that this area is characterized by normal faulting due to extensional regime in the study area. Seismic inline 375 and 460 with marked horizons and faults are shown below in Figure 3.3 and 3.4 to show the geological structure in the study area.

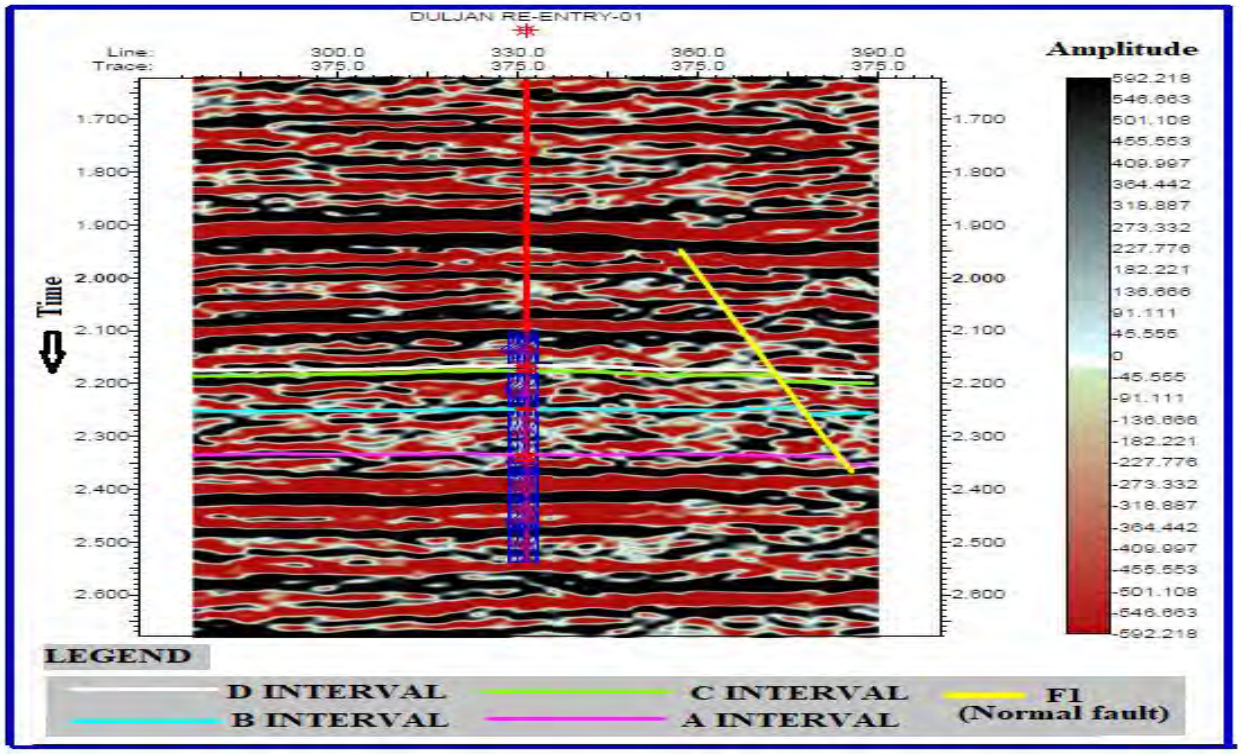

Figure 3.3: Interpreted inline 375 by using synthetic seismogram generated from DULJAN RE-ENTRY-01 well for seismic to well tie

In Figure 3.3, the Lower Goru intervals such as A, B, C and D are marked, and a fault is picked. These horizons are marked based on seismic to well tie using the DULJAN RE-ENTRY-01 well. Although all the horizons appear to be horizontally flat following the law of horizontality, this prevails in an ideal situation. In this study this appears because the studied seismic cube has very small dimensions and does not show the regional trend. The marked fault is a normal fault as the study area is present in the extensional tectonic regime.

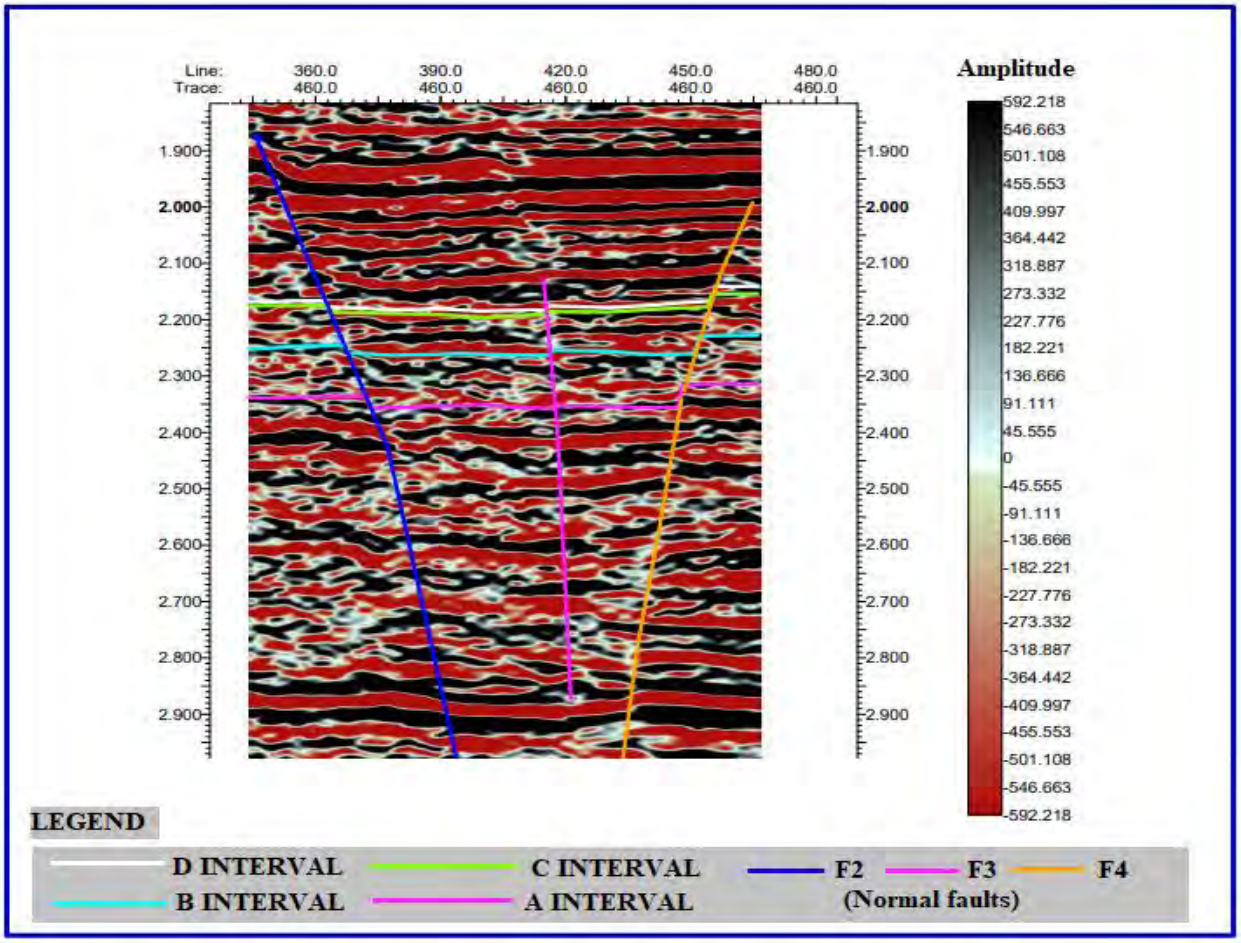

Figure 3.4: Interpreted inline 460 showing major faults in the study area.

In Figure 3.4, the Lower Goru intervals denoted as A, B, C, and D have been delineated along with the identified faults, referencing the DULJAN RE-ENTRY-01 well for seismic-to-well correlation. While these horizons seem to exhibit a horizontal flatness characteristic of the law of horizontality, it's crucial to note that this observation is based on the limited dimensions of the seismic cube used in this study, which may not fully capture the regional geological trends. The faults marked in the figure are interpreted as normal faults, reflecting the extensional tectonic setting of the study area.

3.2.4 Fault polygon generation

Fault polygons of four faults of intervals of lower Goru Formation are marked on base map.

3.2.5 Contour map

Contour mapping is constructing lines of equal values on the map for the available data on the map. Nowadays different software has been used for the generation of contour maps. In my thesis, Kingdom software is used to generate all the contour maps.

There are two types of contour maps used for Seismic Structural Interpretation.

- Time contour map
- Depth contour map

3.2.5.1 Contour map generation of intervals of Lower Goru Formation

The intervals of Lower Goru Formation are main zone of interest in the study area so are marked on seismic sections and the corresponding faults (F1, F2, F3, F4) are also marked intersecting these horizons. Four fault polygons are marked for the corresponding F1, F2, F3 and F4 faults on contour maps. All faults marked on the seismic sections are normal faults and form horst and graben structures due to extensional regime in northeast- southwest direction in the study area. The same structure style is observed on all contour maps of four intervals.

3.2.5.1.1 Time and depth contour maps of A interval

The overall values of time and depth contours of A interval are lower in northeast as compared to southwest direction as shown in Figures 3.5 and 3.6 below.

In figure 3.5, time values of map of A interval shows that as we move from southwest to northeast direction a decline in time values can be observed at F1 fault polygon(yellow) further proceeding at F2 fault polygon(blue) a sharp decline in time values can be observed, further a small increase in time values are observed at F3 fault polygon(pink). A sharp increase in values of time are observed at F4 fault polygon(brown) as we move from F3 fault polygon towards F4 fault polygon.

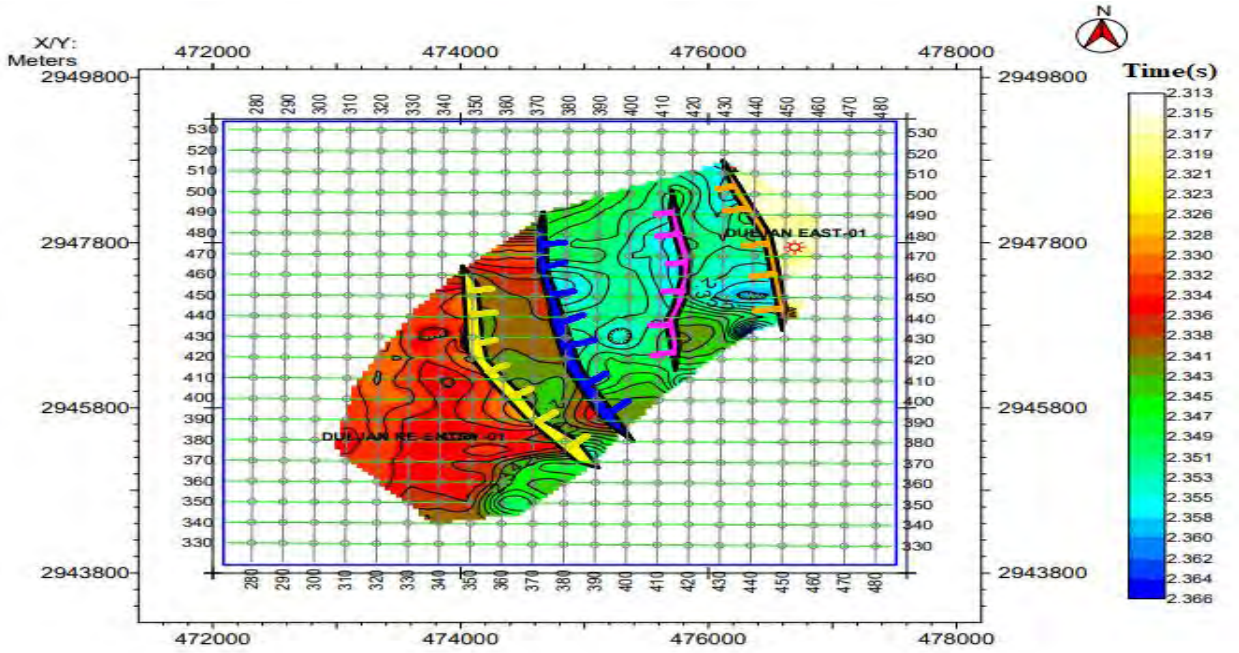

Figure 3.5: Contour map of time for A interval depicting horst and graben structure.

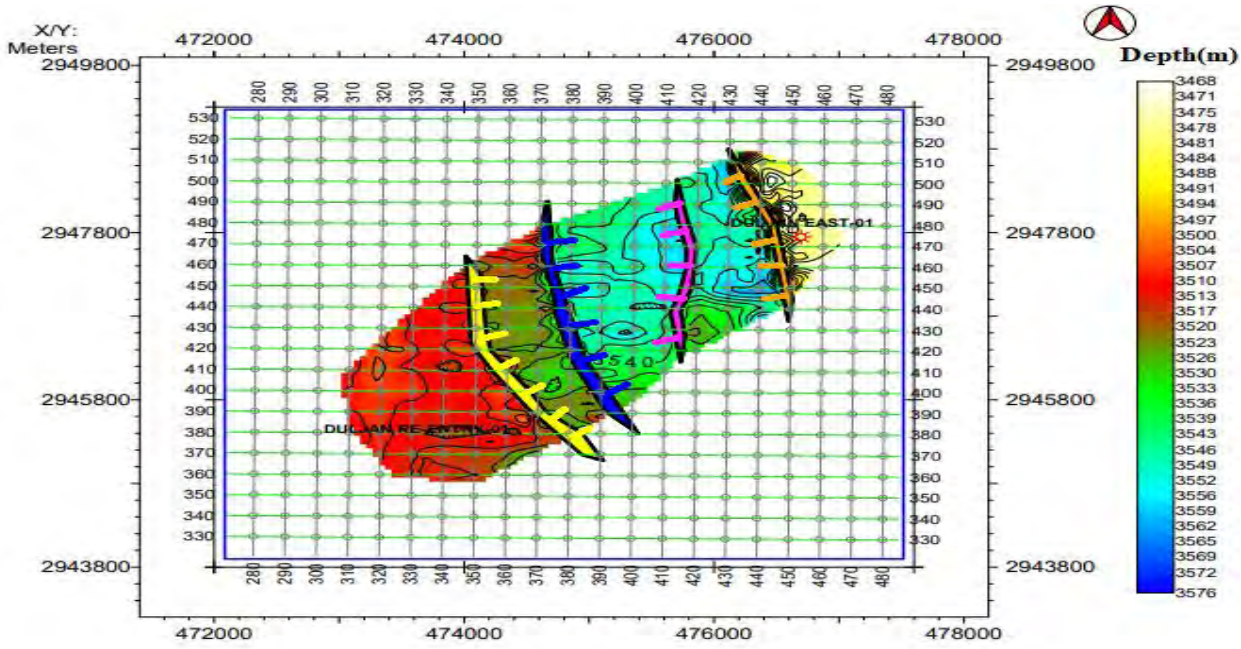

Figure 3.6: Contour map of depth for A interval depicting horst and graben structure.

In figure 3.6, the map of the A interval exhibits a pattern where depth values decrease gradually from southwest to northeast at the F1 fault polygon (yellow), followed by a sharper increase at the F2 fault polygon (blue). Moving from F2 to F3, there is a slight decrease in depth values at the F3 fault polygon (pink), while a notable decrease is observed as we progress towards the F4 fault polygon (brown) from F3.

3.2.5.1.2 Time and depth contour maps of B interval

The values of time and depth contours of B interval are lower in northeast as compared to southwest direction as shown in Figures 3.7 and 3.8 below.

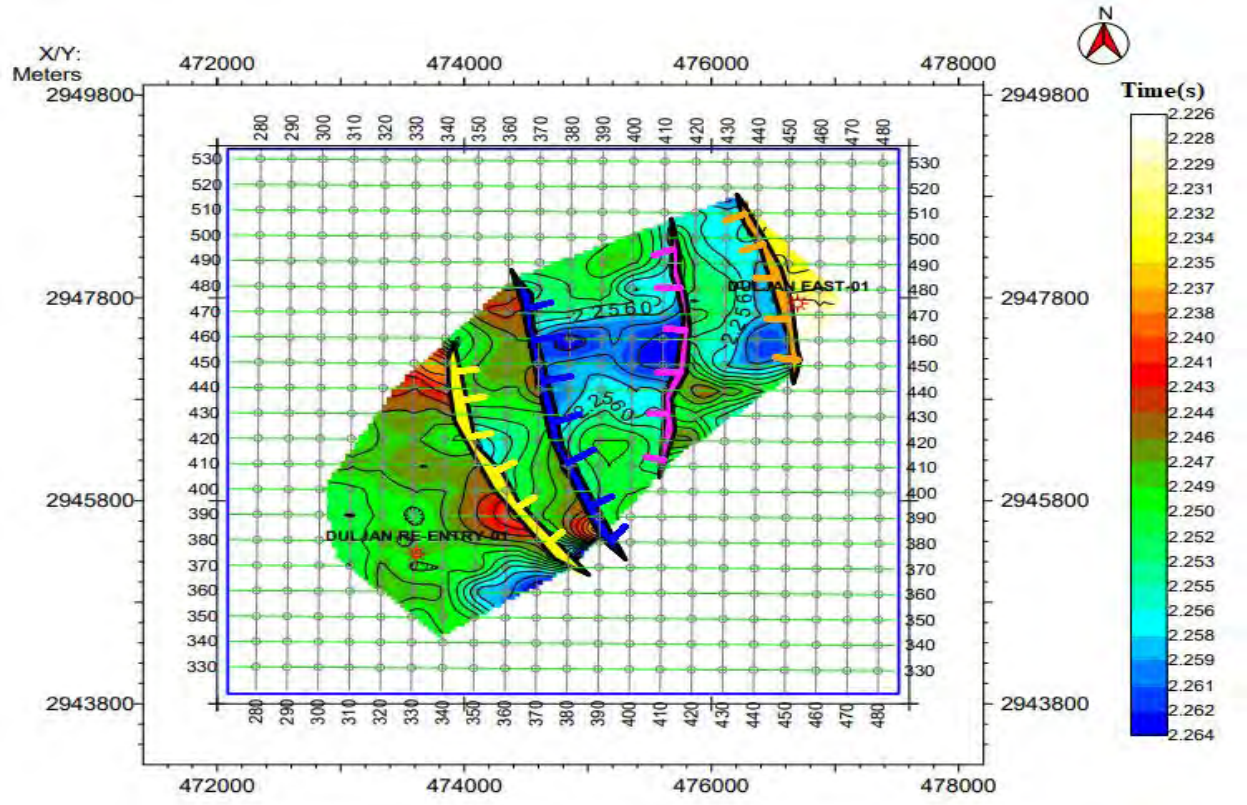

Figure 3.7: Contour map of time for B interval depicting horst and graben structure.

Time and depth values of maps of B interval shows that as we move from southwest to northeast direction an increase in time and depth values can be observed at F1 fault polygon(yellow) and further proceeding at F2 fault polygon(blue) a sharp increase in time and depth values can be observed, further a small decrease in depth and time values are observed at F3 fault polygon(pink).

A sharp decrease in values of depth and time are observed at F4 fault polygon(brown) as we move from F3 fault polygon towards F4 fault polygon.

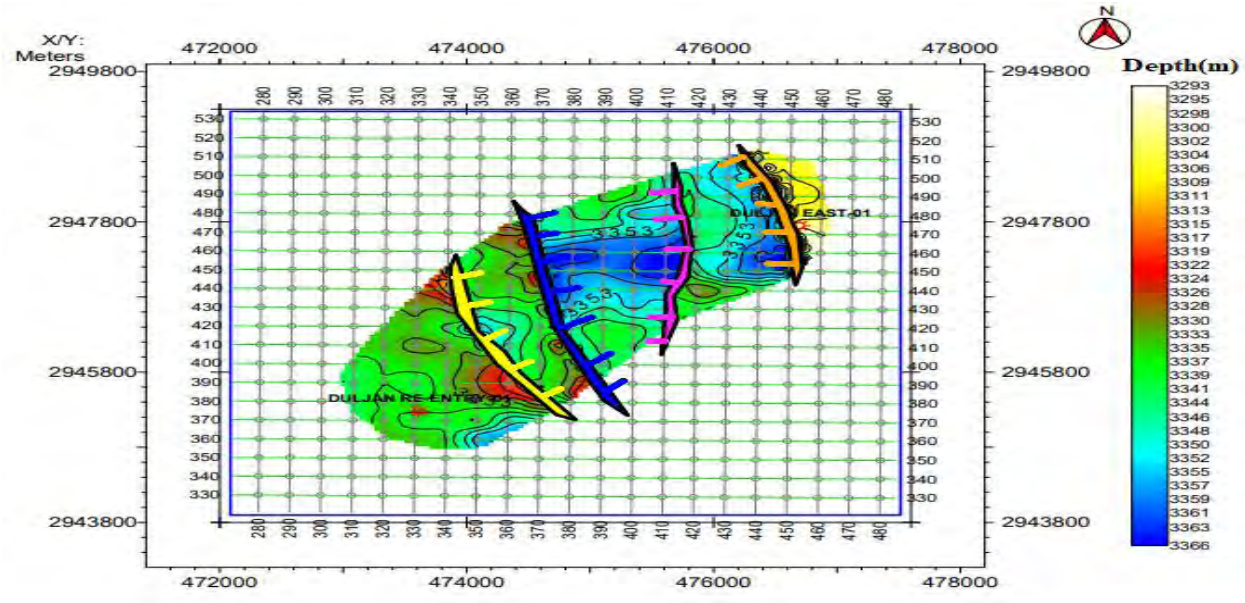

Figure 3.8: Contour map of depth for B interval depicting horst and graben structure

3.2.5.1.3 Time and depth contour maps of C interval

The values of time and depth contours of C interval are lower in northeast as compared to southwest direction as shown in figures 3.9 and 3.10 below.

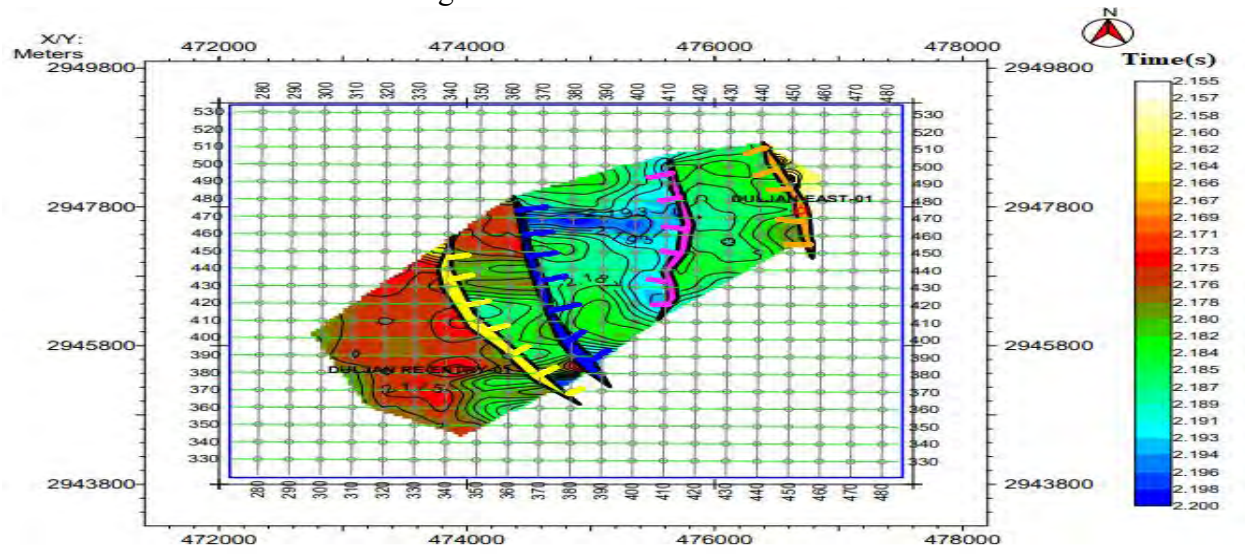

Figure 3.9: Contour map of time for C interval depicting horst and graben structure.

Time and depth values of maps of C interval shows that as we move from southwest to northeast direction an increase in time and depth values can be observed at F1 fault polygon(yellow) and further proceeding at F2 fault polygon(blue) a sharp increase in time and depth values can be observed, further a small decrease in depth and time values are observed at F3 fault polygon(pink) A sharp decrease in values of depth and time are observed at F4 fault polygon(brown) as we move from F3 fault polygon towards F4 fault polygon.

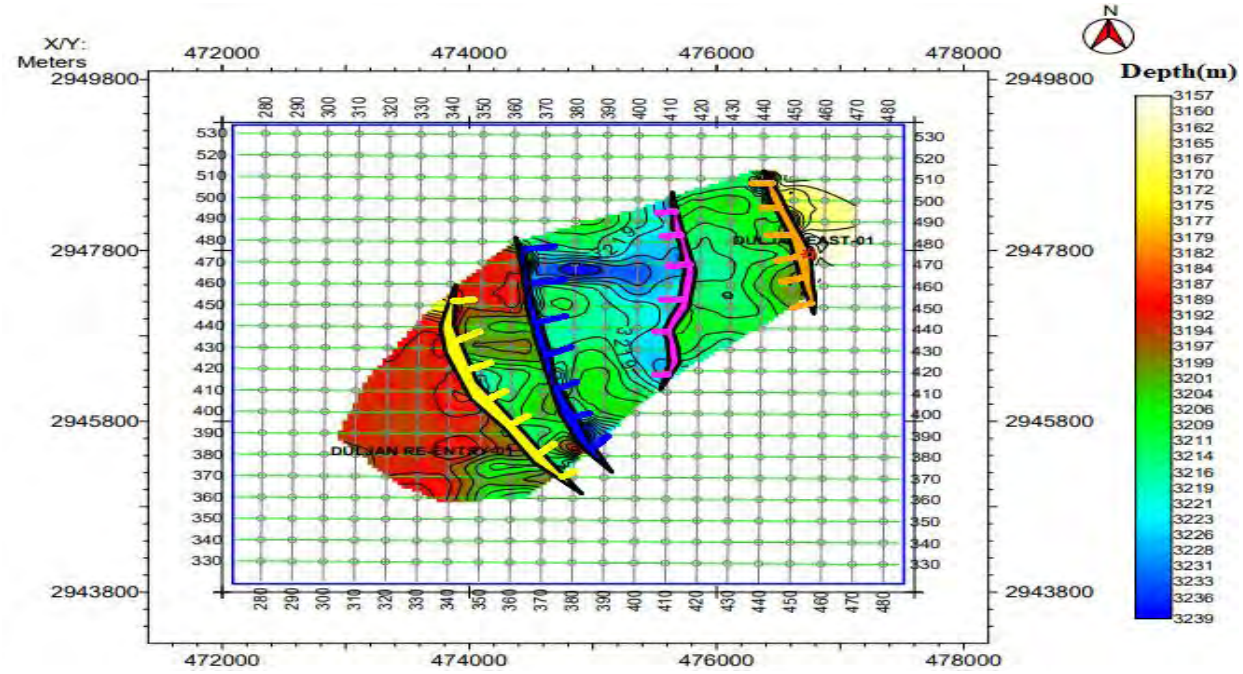

Figure 3.10: Contour map of depth for C interval depicting horst and graben structure.

3.2.5.1.4 Time and depth contour maps of D interval

The values of time and depth contours of D interval are lower in northeast as compared to southwest direction as shown in figures 3.11 and 3.12 below. Time and depth values of maps of D interval shows that as we move from southwest to northeast direction an increase in time and depth values can be observed at F1 fault polygon(yellow) and further proceeding at F2 fault polygon(blue) a sharp increase in time and depth values can be observed, further a small decrease in depth and time values are observed at F3 fault polygon(pink)as we move from F2 towards F3

fault polygon. A sharp decrease in values of depth and time are observed at F4 fault polygon(brown) as we move from F3 fault polygon towards F4 fault polygon.

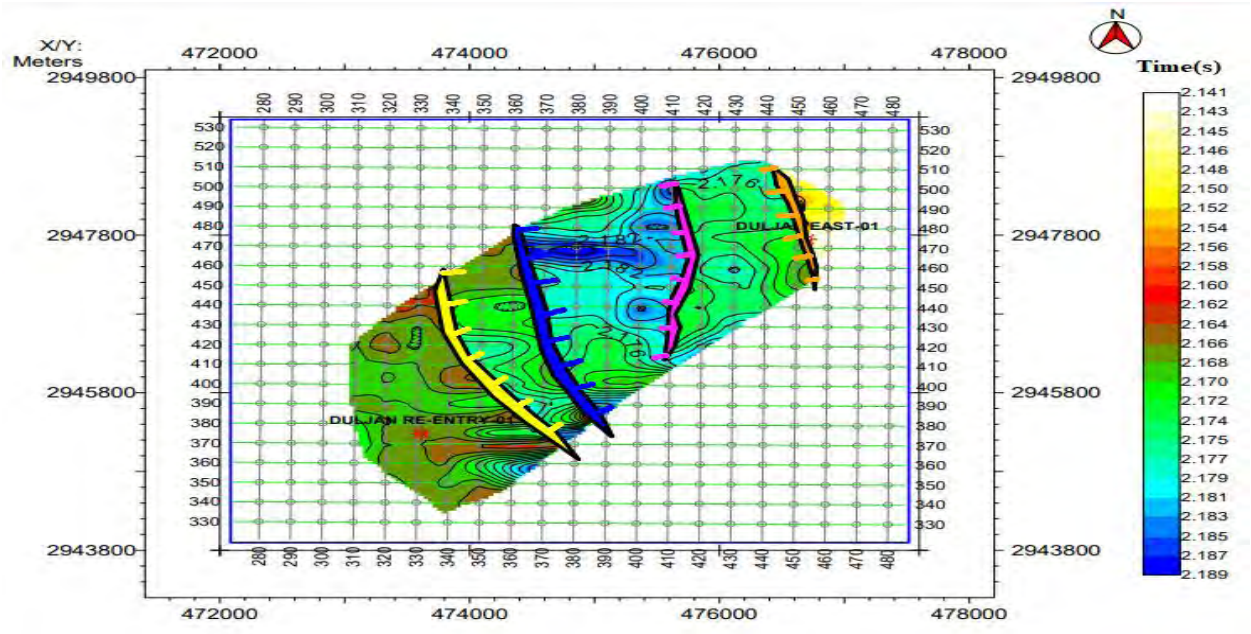

Figure 3.11: Contour map of time for D interval depicting horst and graben structure.

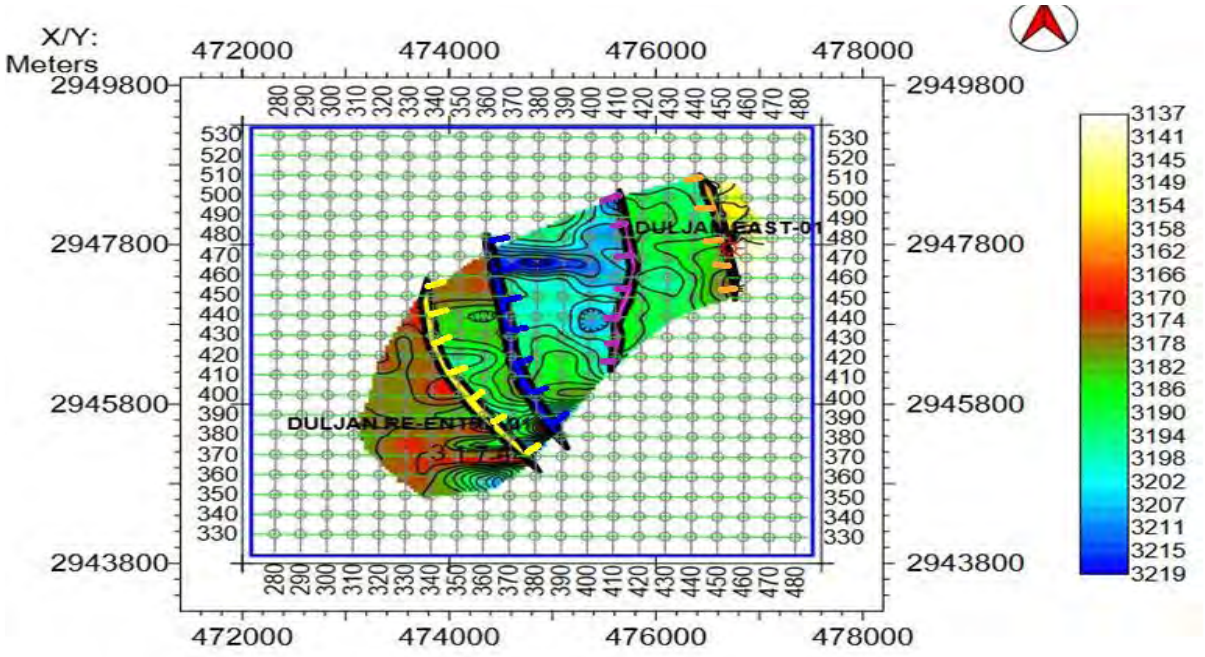

Figure 3.12: Contour map of depth for D interval depicting horst and graben structure.

Chapter No.4 Petrophysical analysis

4.1 Introduction

Petrophysical log analysis plays a vital role in reservoir modeling and is considered a fundamental tool to initially interpret the lithology and fluid types that lies within various reservoir zones (Ali et al., 2015). The main purpose of petrophysical analysis is to obtain petrophysical parameters of reservoirs rock such as volume of shale, porosities (density porosity, total porosity, effective porosity), hydrocarbon saturation to mark zone where possible hydrocarbons may be present. The reservoirs can be analyzed for hydrocarbon accumulation in both qualitative and quantitative ways. For qualitative analysis, the scanning of wire line log-data is involved to predict the hydrocarbon signatures such as high resistivity, low spontaneous potential, low gamma ray and low-density log values. In quantitative analysis petrophysical parameters are calculated. The first step of analysis is logging conditioning in which the data values (that show anomalous deviation) are edited properly to establish a trend against depth. Petrophysical analysis of DULJAN RE-ENTRY-01 and DULJAN EAST-01 wells of DULJAN block, Khairpur, Sindh, Lower Indus Basin are carried out to delineate the petrophysical properties of Lower Goru intervals.

The petrophysical analysis is carried out by using the following wire line logs.

- Density Log
- Neutron Log
- Sonic log
- Spontaneous Potential
- Resistivity Logs
- Caliper Log
- Gamma ray

4.2 Workflow for petrophysics

The workflow for the petrophysical analysis is shown below:

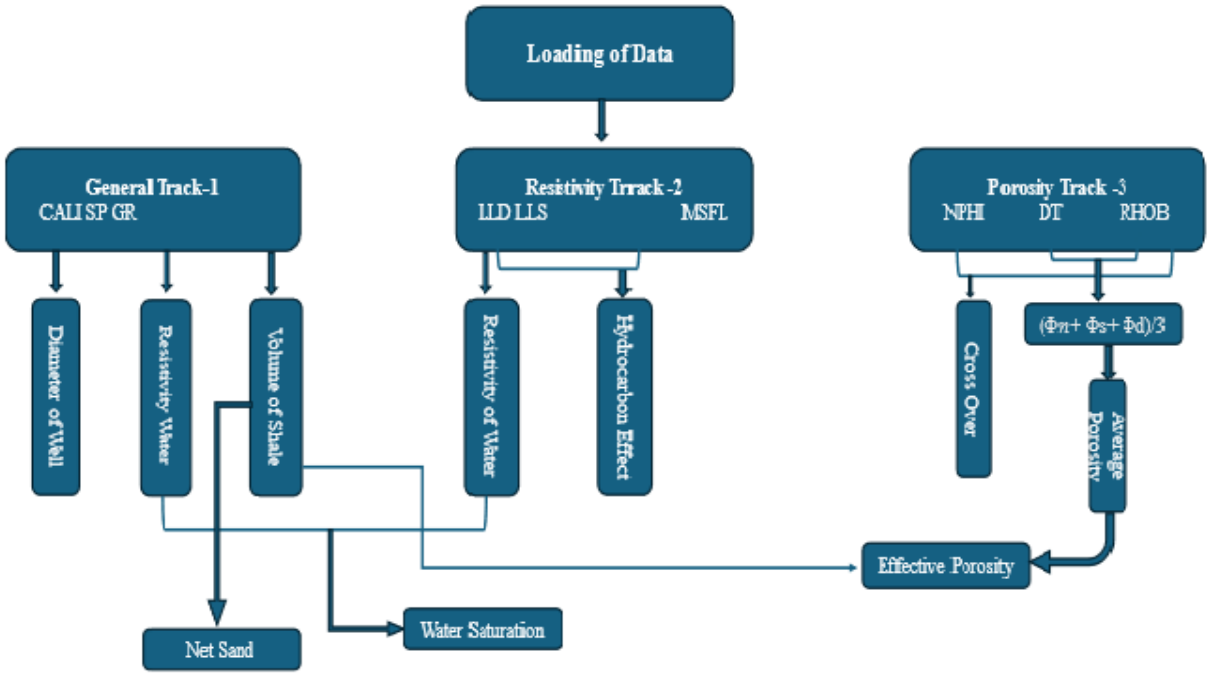

Figure 4.1: Workflow for the petrophysical analyses.

This workflow started from the well loading, then defining the tracks, there are different tracks shown in Figure 4.1. After defining tracks, we select specific logs in specific tracks, like in lithology track we select GR, SP and CAL. After selection of logs, we compute different petrophysical parameters like volume of shale, porosities etc.

4.3 Description of the Logs

Classifications of different logs with some short descriptions are given as follows. We defined different tracks for different logs.

4.3.1 Lithology Track

Lithology track also known as general track 1 contains the following three logs.

- GR log
- SP log
- CAL log

4.3.1.1 Gamma Ray Log

It is represented as GR log. This is one of the main logs used for the identification of lithology. It measures the natural radioactive contents, emitted from a formation. Usually, it is used for the identification of sand and shale delineation. In practice, shale has the highest gamma ray value than other sedimentary rocks because it emits many gamma ray radiations. In common practice, sometimes non-shale content also gives the gamma rays radiation because sandstone may contain uranium, potassium feldspar, clay fillings or rock pieces.

4.3.1.2 Spontaneous Potential

Spontaneous potential (SP) records the naturally occurring potential in the well bore. In this we have two electrodes, moving and static electrodes. Moving electrode is dragged into the borehole while static is on the surface as a reference. Through SP log potential difference is measured between static electrode and moving electrode in the borehole. (Asquith and Gibson, 2004). There are following utilization of this log.

1. For the delineation of permeable zones (sand) and impermeable zone (Shale).
2. Detect boundaries of beds.
3. Determine volume of shale in impermeable beds.
4. Determine resistivity of formation water.
5. Qualitative measure of permeability.

4.3.1.3 Caliper Log

It is represented as CAL. In the exploration of hydrocarbons, it's necessary to determine the size (diameter) of the bore hole. Caliper log is used for this purpose. This log also helps us to determine the shape of the bore hole as well. The presence of clay in the borehole causes swelling and caving which give false readings, so diameter and shape should be known for the quantitative measurements of the reservoir.

4.3.2 Resistivity Track

This is the second track. In this track we run the resistivity logs (LLD, LLS & MSFL) and we try to find the cross-over between LLD and LLS, for the prediction of fluid presence.

4.3.2.1 Laterolog Shallow

It is represented as LLS. It is used for the investigation of transition zones. It has smaller investigation depth than LLD. With the help of this log, we can find the resistivity of flushed ($Rx0$) and transition (Ri) zones.

4.3.2.2 Laterolog Deep

It is represented as LLD. Laterolog deep is used for the investigation of deep uninvaded zones (undisturbed zone). An uninvaded zone is the zone beyond the invaded zone where the formation's fluids are present in pure form without any penetration of mud filtrate. This log is used for both saline and fresh mud. This log gives the true resistivity of the reservoir (Rt) and fluid (Rw). It has deep penetration as compared to the (LLS). Figure 4.2 shows the different zones round boreholes with the resistivity.

Flushed zone is the zone where fluid present in pores is replaced by mud filtrate. In this, we have resistivity of mud cake. **Invaded zone** is that in which we have both mud and fluids in the pores of the rock, in this zone resistivity of mud filtrate can be found. **An uninvaded zone** is the zone in which we have pure fluids in the pores, the true resistivity i.e. water and hydrocarbon resistivity can be found in this zone with the help of LLD log. Borehole zones are shown in Figure 4.2 below.

4.3.3 Porosity Track

This is the third track and is an important track in determining the reservoir characteristics. In this, we display formation density log (RHOB), sonic log (DT) and neutron porosity log (NPHI). In this log, we are also trying to find the cross-over between RHOB and NPHI, DT as a support. This cross-over is very important because from this we can predict the type of fluid in the reservoir. From these logs, we can find the effective porosity of the interest zone. Neutron log, density logs

and sonic logs are the porosity logs. None of these logs gives direct porosity values. We can find the porosity of the formation by analyzing these logs.

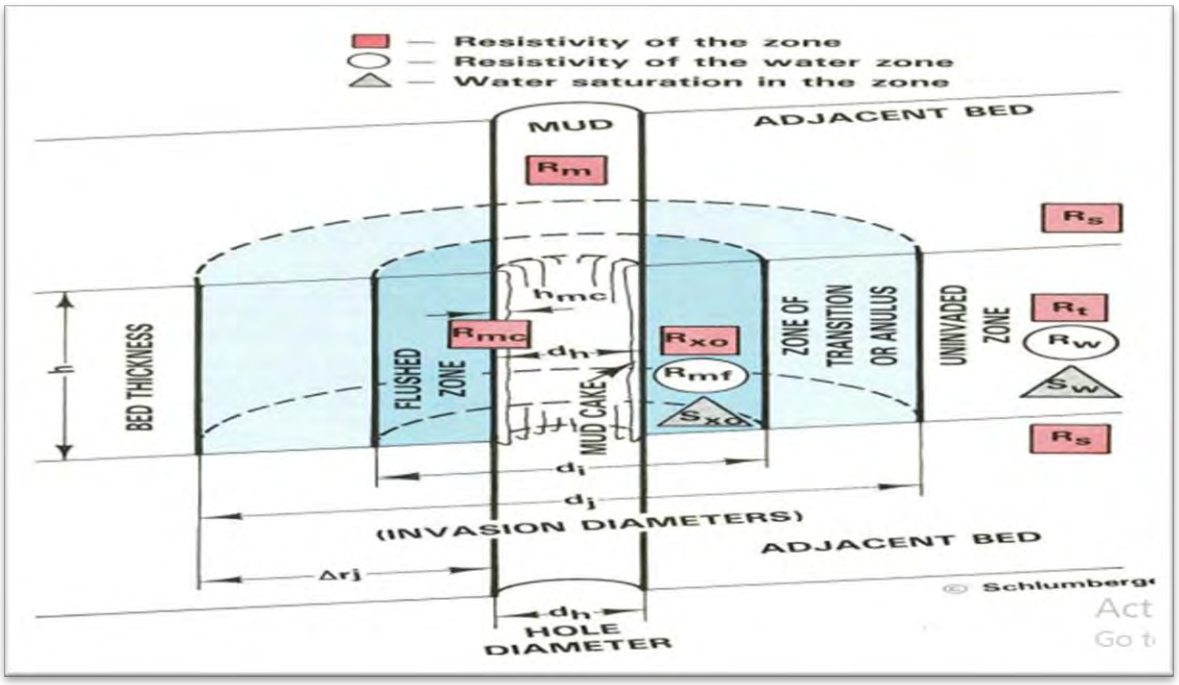

Figure 4.2: Schematic diagram of borehole zones (Schlumberger)

4.3.3.1 Density Log

Density log (RHOB) displays the electron density of formation in contact by detecting the scattered gamma rays. It gives an indication of porosity, lithology and can assist to detect gas bearing zones. Neutron and density log cross over is an indicator of Gas/hydrocarbons called Gas Effect. The overlapping curves indicate the presence of water.

4.3.3.2 Sonic log

In Sonic log sound waves interval transit time is measured. It is a porosity log. Sonic log is recorded by putting a tool in borehole by wireline. This tool emits sound waves that travels from the source to the formation and recorded back on the receiver. For porous rock the travel time increases and hence the larger deflection occurs on the log display and for denser and nonporous material the traveling velocity increases and hence the travel time decreases.

4.3.3.3 Neutron log

Neutron log is based on the effect of the lithology on fast moving neutrons emitted by a source. Hydrogen has the largest effects on these neutrons in slowing down and absorbing them. Since hydrogen is found in water and hydrocarbons. This is found mainly in pores, so neutrons are a direct indicator of porosity. Where the neutron porosity value is low, it may be an indicator of hydrocarbon presence.

4.4 Petrophysical parameters

Petrophysical parameters refer to the physical properties of rocks and fluids in the subsurface, crucial for understanding reservoir characteristics in the oil and gas industry. These parameters include porosity, permeability, and fluid saturation, influencing the flow of hydrocarbons in reservoirs.

4.4.1 Lithology identification

Lithology identification is a significant parameter in petrophysical analysis and is important because other petrophysical parameters depends on lithology. Gamma ray (GR) and photoelectric factors (PEF) logs are used in Lithology identification.

4.4.2 Fluid identification

Fluid identification is important in petrophysical analysis. Fluid present in the reservoir is identified by LLD-LLS and RHOB-NPHI crossovers. Where hydrocarbons are present LLD resistivity is higher than LLS resistivity because LLD gives formation true resistivity and LLS show resistivity of mud filtrate, hydrocarbons have higher resistivity than water so where hydrocarbons are present in the formation LLD log is on the right side of LLS. RHOB and NPHI indicate the fluid type by showing large crossover separation for gas presence and smaller crossover separation for oil.

4.4.3 Volume of shale (Vsh)

Vsh calculation is also important in petrophysical analysis because it tells about reservoir and non-reservoir zone by identifying lithology and porosity depends on it. Linear formula for Vsh calculation is given below in equation (4.1) (Islam et al., 2013):

$$IGR = \frac{GRlog - GRmin}{GRmax - GRmin} \quad (4.1)$$

Where, IGR = gamma ray Index, $GRlog$ = gamma ray on log

$GRmin$ = minimum GR, $GRmax$ = maximum GR

There are other formulas also for volume of shale calculations applied according to condition.

4.4.4 Porosity

Porosity is also important in petrophysical analysis. Porosity is the ratio of void spaces present in rock to the total volume of rock. Total porosity and effective porosities were calculated below:

4.4.4.1 Total porosity calculation

Neutron–density logs are used to estimate total porosity. Neutron density porosity can be computed from the equation (4.2) given below:

$$\Phi total = \frac{\Phi N + \Phi D}{2} \quad (4.2)$$

Where, Φ_N=Neutron porosity

Φ_D = porosity through density, calculated from equation (4.3) given below (Dolan P, 1990):

$$\Phi D = \frac{\rho ma - \rho b}{\rho ma - \rho f} \quad (4.3)$$

Where, ρb = bulk density (fluid +rock density) (RHOB log reading)

ρf =density of fluid present in rock, ρma = rock matrix density

4.4.4.2 Determination of effective porosity

Effective porosity is the porosity of total number of pore spaces interconnected with each other. Effective porosity is always less than total porosity and depends on total porosity and volume of shale present in reservoir rock. Effective porosity can be calculated from the following equation (4.4). (Atlas, 1979):

$$\Phi eff = \Phi total * (1 - Vsh) \quad (4.4)$$

Where, $\emptyset eff$ = effective porosity, $\Phi total$= total porosity, Vsh = Shale volume.

4.4.5 Water saturation (Sw)

Sw is the percentage of water present in interconnected pore spaces. To calculate water saturation effective porosity and deep resistivity logs are used. Hydrocarbon saturation also depends on water saturation of reservoir rock. Water saturation can be calculated from archie's equation (4.5) given below. (Archie, 1942):

$$Sw = [\frac{(a*Rw)}{(Rt*\Phi_m)}]^{\frac{1}{n}} \quad (4.5)$$

Where, Sw = water saturation in reservoir rock, a = tortuosity, n = saturation exponent, Rw = formational water resistivity, φ =effective porosity, m = cementation factor, Rt = true formational resistivity.

4.4.6 Hydrocarbon saturation (HS)

The HS of reservoir rock directly depends on its water saturation. Hydrocarbon saturation percentage is calculated by subtracting water saturation percentage from 100. Formula is given below (4.6):

$$HS = 100 - Sw \quad (4.6)$$

4.5 Petrophysical results of DULJAN RE-ENTRY-01 and DULJAN EAST-01 wells

Zones of interests marked based on composite log response for DULJAN RE-ENTRY-01 and DULJAN EAST-01 wells are shown in Figure 4.3 and 4.4 below: 4.3 and 4.4 below:

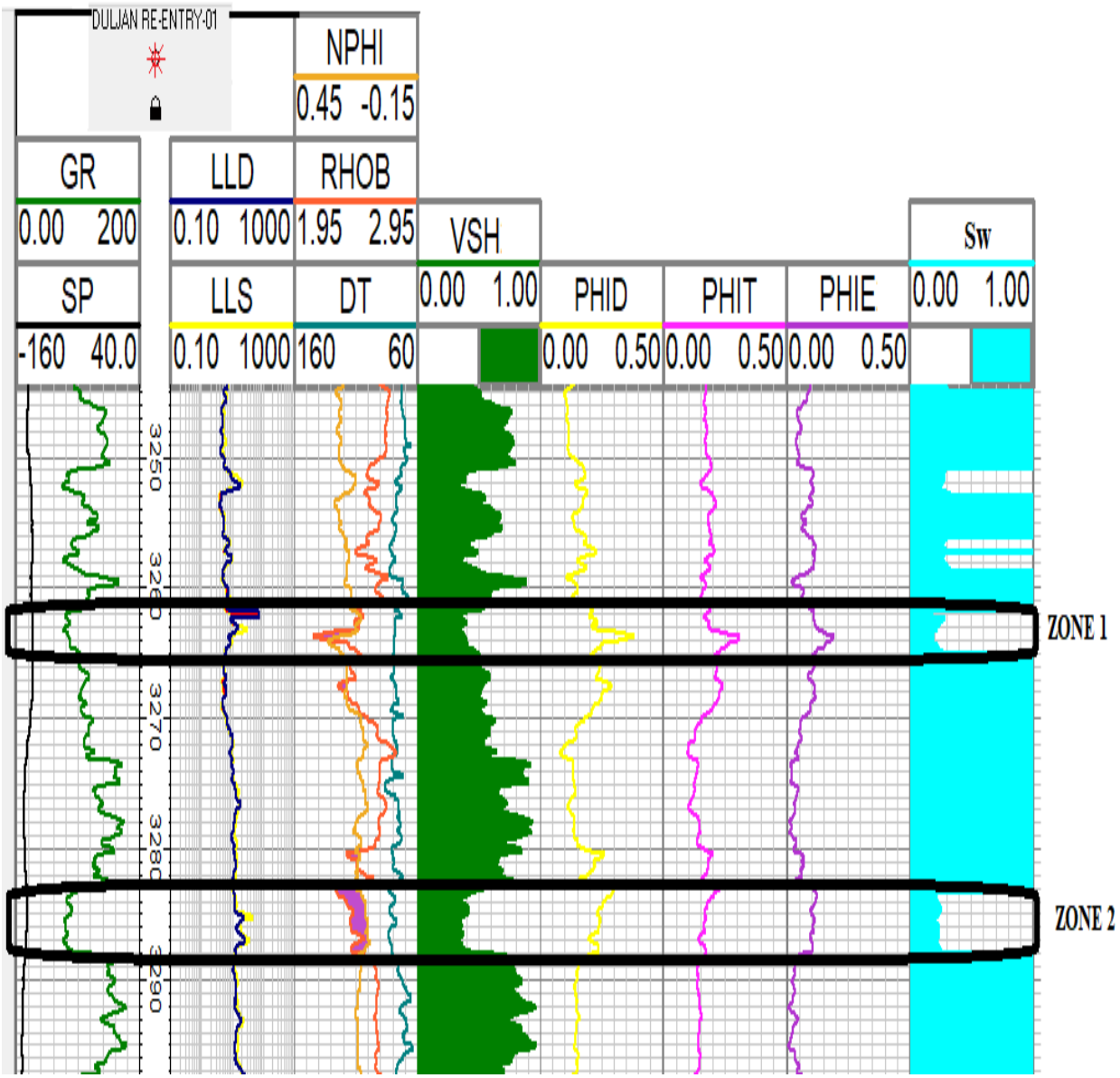

Figure 4.3: Zone of interests marked on the basis of composite response of logs on DULJAN RE-ENTRY-01 well.

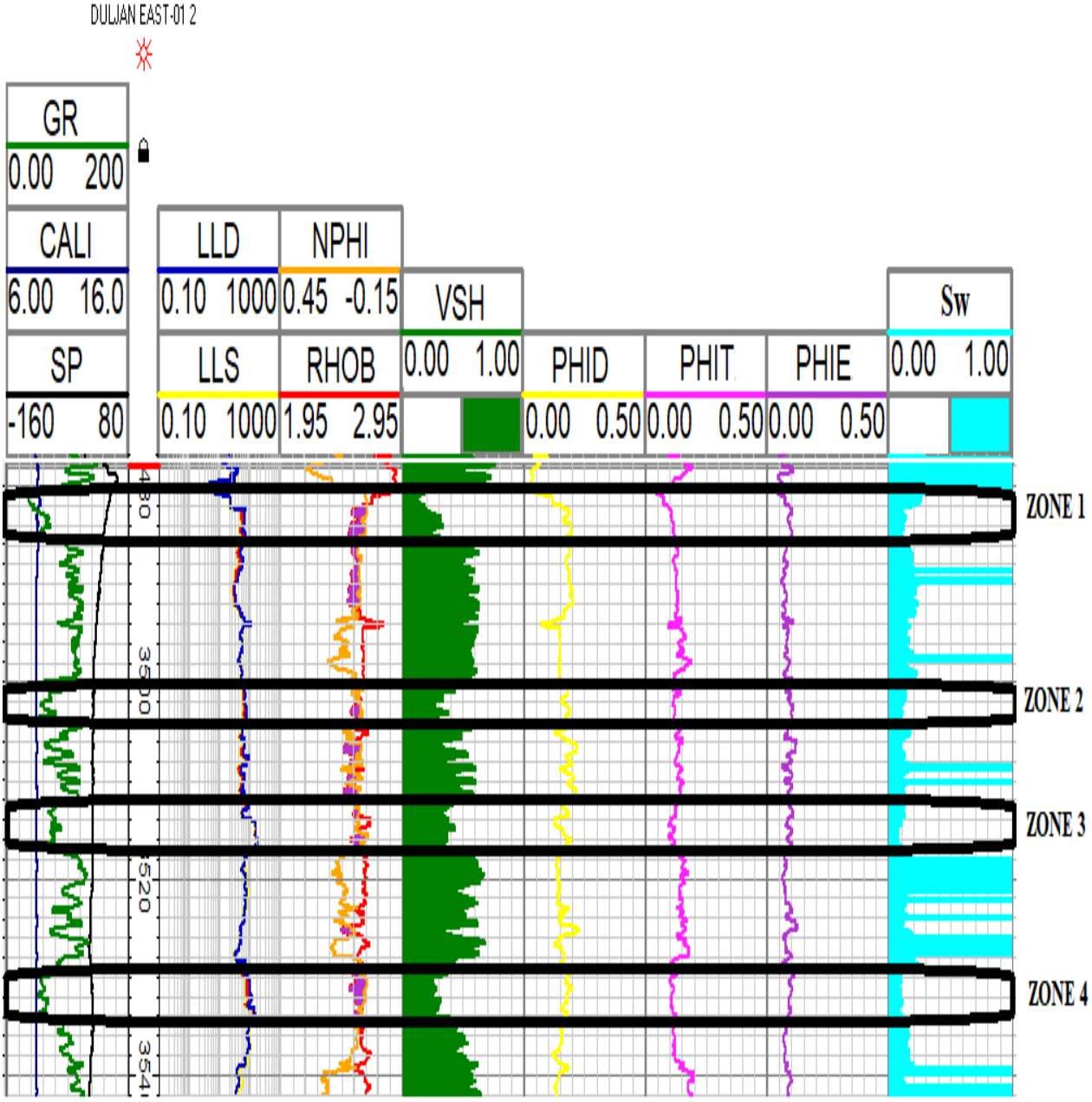

Figure 4.4: Zone of interests marked on the basis of composite response of logs on DULJAN EAST-01 well.

There are two zones of interest marked on DULJAN RE-ENTRY-01 well and four zones on DULAJN EAST-01 well based on composite response of logs and the petrophysical parameters estimated from these logs. Depths at which zone of interests are marked have low values of gamma

ray, LLD and LLS separation, low density, low neutron porosity, stable caliper, low SP, higher values of DT, porosities, and low water saturation. Two zones marked in DULJAN RE-ENTRY-01 well lie in C interval sands. Zone 1 has a thickness of three meters(3262-3265m) and zone 2 has thickness of five meters ranging from (3283-3288m). DULJAN RE-ENTRY-01 well status is abandoned, it has two zones of interests, but the thickness of both zones is very small. Four zones marked in DULJAN EAST-01 well lie in A sand interval. Zone 1 has a thickness of six meters(3480-3486m) and zone 2 has a thickness of four meters(3500-3504m), Zone 3 have thickness of five meters(3512-3517m) and Zone 4 have thickness of six meters(3528-3534m). DULJAN EAST-01 well status is gas well. Averages calculated for petrophysical parameters in zones of interests for DULJAN RE-ENTRY-01 and DULJAN EAST-01 wells are shown in table 4.1 below.

Table 4.1: Table showing averages of calculated petrophysical parameters for zones of interests of DULJANRE-ENTRY-01 and DULJANEAST-01 wells.

Well	**Vsh (%)**	**Density porosity (%)**	**Total porosity (%)**	**Effective porosity (%)**	**Sw (%)**
DULJAN RE-ENTRY-01 (Zone one)	40	24	21	12	36
DULJAN RE-ENTRY-01 (Zone two)	41	23	17	10	40
DULJANEAST-01 (Zone one)	28	14	9	7	27
DULJANEAST-01 (Zone two)	33	17	11	9	12
DULJANEAST-01 (Zone three)	37	16	11	9	10
DULJANEAST-01 (Zone four)	33	16	11	9	14

4.6 Facies analysis

Facies analysis is a fundamental approach to identify lithologies present in the area with the help of log responses of wells. Facies analysis is very significant because reservoir rock properties directly depend on lithology. Facies analysis is also very significant in sequence stratigraphic studies, as well as for defining improved reservoir rock characterization.

4.6.1 RHOB, NPHI and GR log cross plots of DULJAN EAST-01 well

RHOB, NPHI and GR logs cross plots of DULJAN EAST-01 well for facies analysis is shown below in Figure 4.5.

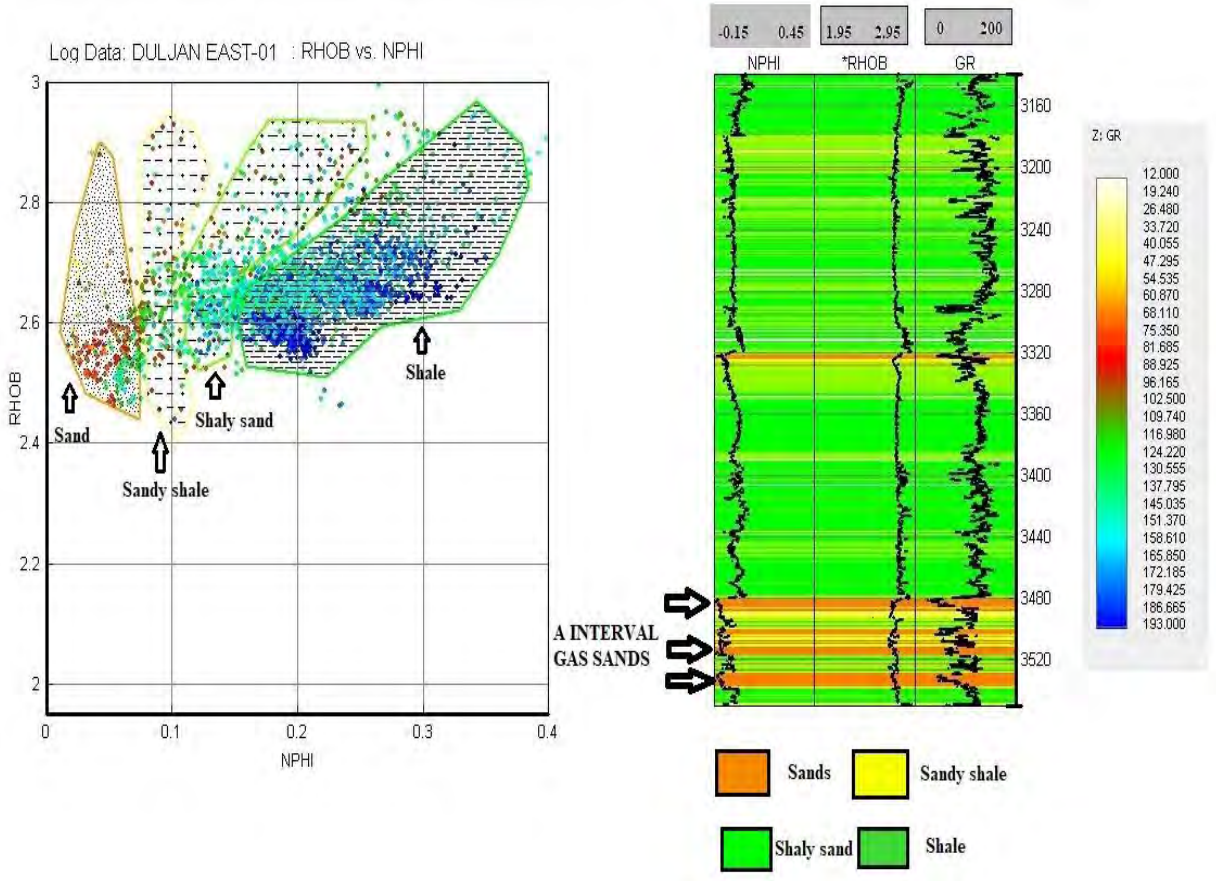

Figure 4.5: Facies analysis of DULJAN EAST -01 well through RHOB, NPHI and GR log cross plots.

Through cross plots of NPHI, RHOB and gamma ray log four lithologies, sands, shales, shaly sands, and sandy shale are identified in four intervals of Lower Goru Formation of DULJAN block. Sand area marked on cross plots have low values of NPHI, RHOB and gamma ray, shale area marked on cross plots have high values of NPHI, RHOB and gamma ray whereas shaly sand and sandy shales have values in between them. Sands marked on NPHI and RHOB cross plots are gas sands also confirmed through petrophysical results because sand lithology shown on NPHI and RHOB logs matches the depth of zone of interests marked in petrophysical analysis. Facies analysis of DULJAN EAST-01 well reveals that A interval sands are the main reservoir and overall intervals of Lower Goru contains thin sand shale layering in which shaly component is dominant than sand lithology.

4.6.2 RHOB, NPHI and GR log cross plots of DULJAN RE-ENTRY-01 well

RHOB, NPHI and GR logs cross plots of DULJAN RE-ENTRY-01 well for facies analysis is shown below in Figure 4.6.

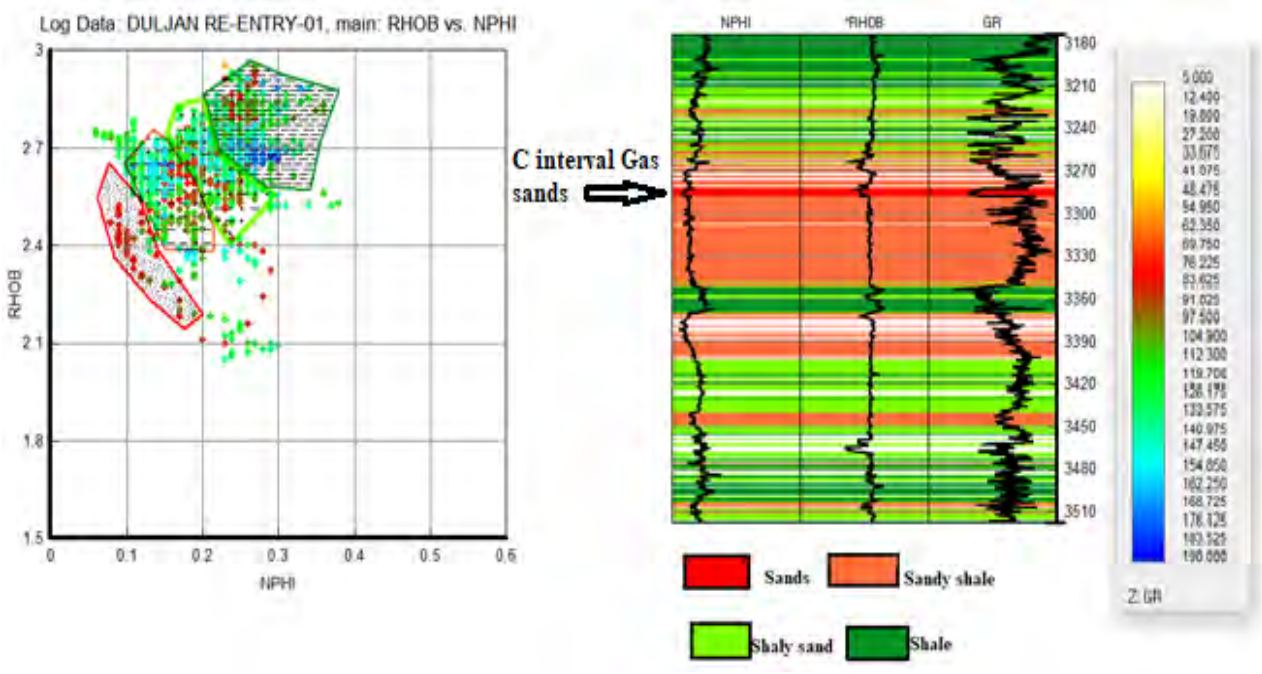

Figure 4.6: Facies analysis of DULJAN RE-ENTRY-01 well through RHOB, NPHI and GR log cross plots

Through cross plots of NPHI, RHOB and gamma ray four lithologies sands, shales, shaly sands, and sandy shale are identified in four intervals of Lower Goru Formation of DULJAN block. Sand area marked on cross plots have low values of NPHI, RHOB and gamma ray, shale area marked on cross plots have high values of NPHI, RHOB and gamma ray whereas shaly sand and sandy shales have values in between them. Sands marked on NPHI and RHOB cross plots are gas sands also confirmed through petrophysical results because sand lithology shown on NPHI and RHOB logs matches the depth of zone of interests marked in petrophysical analysis. Facies analysis of DULJAN RE-ENTRY-01 well reveals that C interval sands are main reservoir and overall intervals of Lower Goru contains thin sand shale layering in which shale component is dominant than sand lithology.

Chapter No.5 Seismic Inversion

5.1 Introduction

Inversion is defined as "From seismic and well data deriving inverted impedance section that best describes the subsurface." (Sheriff, 2002). In inversion with integration of seismic and well data, inverted impedance sections are generated which also gives lateral continuous information which cannot be obtained from only well data because well data gives information of subsurface only at a single point.

Acoustic impedance is obtained by convolving P-wave and density logs. Inversion is the reverse of forward modelling. From seismic data a wavelet is extracted which turns it into reflection coefficient series, these reflection coefficients are then converted to acoustic impedance sections with the help of Zoeppritz equation. From acoustic impedance sections zone of interest shows low impedances and its lateral extend can be seen. Nowadays inversion techniques are widely used for hydrocarbon exploration. Different inversion techniques are used for improved reservoir characterization, all of which have different specifications and applied according to subsurface conditions.

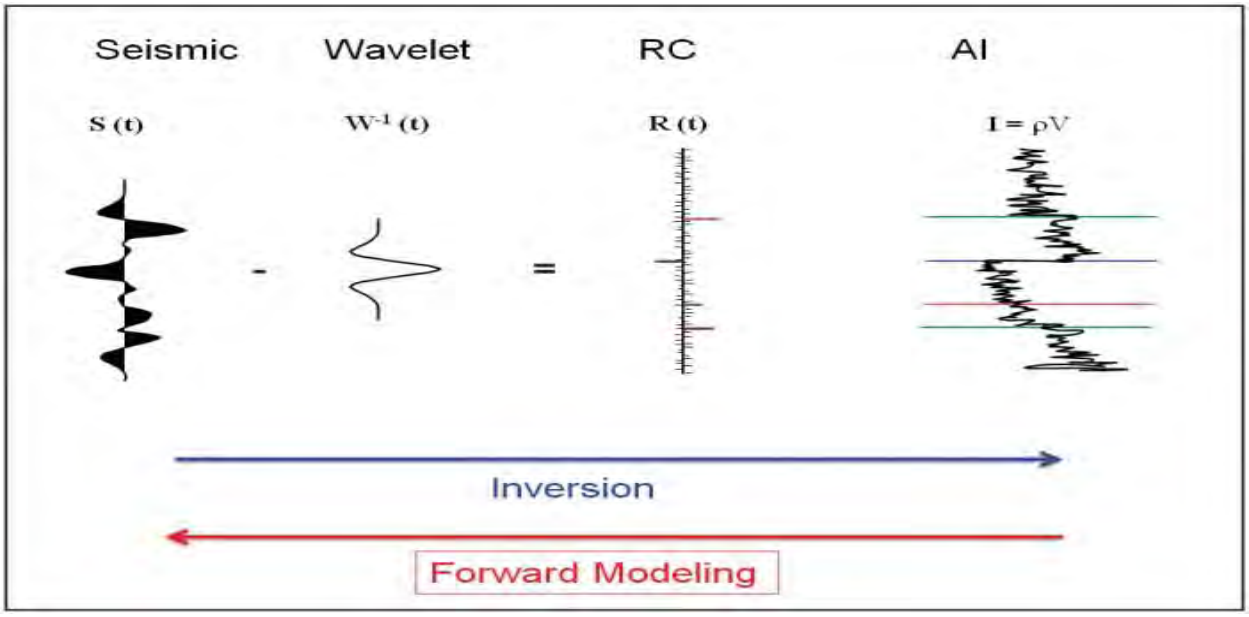

Figure 5.1: Workflow for inversion and forward modeling process

5.2 Types of Inversion

Types of Inversion methods for post-stack data are listed below:

- Recursive inversion (trace integration)
- Sparse-spike inversion (SSI)
- Least-squares inversion
- Band limited inversion
- Sparse layer reflectivity inversion
- Model based inversion
- Colored inversion

In our study, we only used two types of inversion i.e. band limited and Sparse layer reflectivity inversion for improved reservoir characterization of DULJAN block, Khairpur area, lower Indus Basin, Pakistan.

5.2.1 Band-limited inversion theory (BLI)

BLI technique simply converts the seismic traces to earth's reflectivity series. The zero offset reflection coefficient can be obtained by equation (5.1) below:

$$r_i = \frac{z_{i+1} - z_i}{z_{i+1} + z_i} \tag{5.1}$$

where r_i is the zero offset reflection coefficient at ith interface, z_i is the impedance of ith layer and z_{i+1} impedance of (i+1)th layer. (i+1)th layer impedance is obtained from equation (5.2), proposed by Lindseth (1979).

$$z_{i+1} = z_i\left(1 + \frac{2r_i}{1 - r_i}\right) \tag{5.2}$$

Impedance of (n+1) th layer can be found from first layer's impedance from equation (5.3) given below.

$$z_{n+1} = z_1 \prod_{k=1}^{i} \left(\frac{1+r_i}{1-r_i}\right) \tag{5.3}$$

Dividing equation (5.3) with Z1 (first layer impedance) and taking logarithm on both sides, equation (5.4) can be obtained.

$$z_{i+1} = z_1 \exp\left(2 \sum_{k=1}^{i} r_k\right) \tag{5.4}$$

Seismic trace modelling as scaled reflectivity (Sk) can be obtained from relation given below in equation (5.5),

$$S_k = \frac{2r_k}{\gamma} \tag{5.5}$$

where γ is the scaling factor and equation (5.5) can be modified as:

$$Z_{i+!} = Z_i \exp\left(\gamma \sum_{k=1}^{i} S_k\right) \tag{5.6}$$

Equation (5.6) gives the results of acoustic impedance.

5.2.2 Sparse layer reflectivity inversion (SLR) theory

Sparse Layer reflectivity inversion is used for layered subsurface geology. Seismic trace is obtained by convolving source pulse with reflection series, source pulse may be Ricker wavelet (Shearer, 2009), and the subsurface reflectivity x ∈ R n, obtained from y = h ∗ x + n, where n is the noise and ∗ is convolution. Reflectivity is modeled as a sparse vector comprising subsurface layers, each layer has constant impedance, which gives piecewise-constant impedance model (Oldenburg & Yilmaz, 2001). Figure 5.2 shows the model with two shale layers and in between them is a wet sand layer (Figure 5.2(a)). (Russell, 2019). Reflectivity (Figure 5.2(c)) convolved with source (Figure 5.2(d)) gives us seismic trace at the receiver (Figure 5.2(e)).

Reflectivity shows subsurface geology (Figure 5.2(a)) from acoustic impedance (Figure 5.2(b)), Acoustic impedance can be obtained by multiplying density and P-wave velocity. (Oldenburg, 1983), obtained from equation (5.7) given below:

$$r_i = \frac{\rho_{i+1}V_{i+1} - \rho_i V_i}{\rho_{i+1}V_{i+1} + \rho_i V_i} \tag{5.7}$$

Least square formulation leads to issue of non-uniqueness due to band limited wavelet in which there is loss of low and high frequencies (Berkhout et al., 1977). The non-uniqueness issue can be solved through regularization. (Oldenburg & Taylor, 1979).

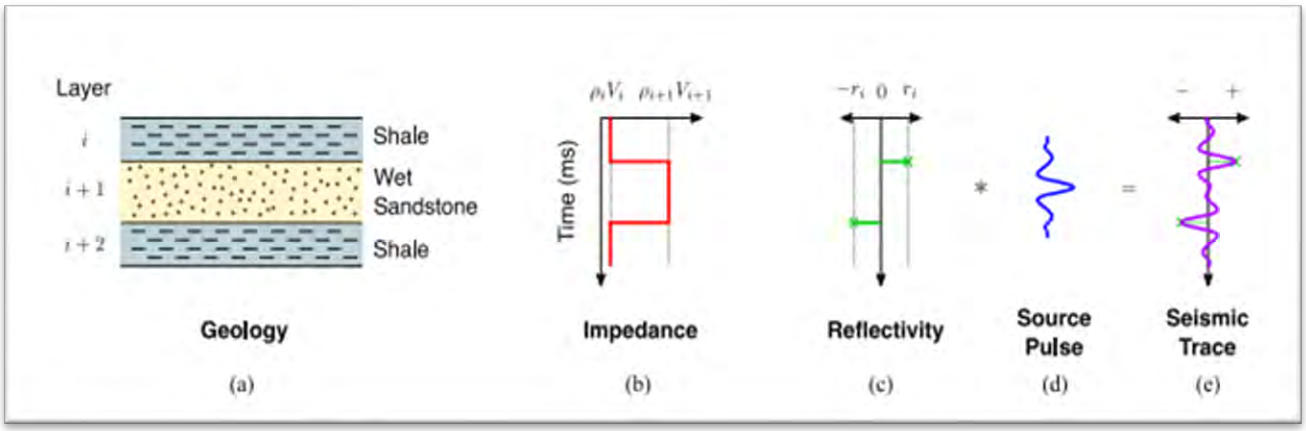

Figure 5.2: Three-layer model.

Sparse layer reflectivity inversion has improved resolution and can detect thin layers from seismic data. The drawback of sparse layer reflectivity inversion is its high computational cost.

5.3 Generalized workflow for post stack inversion

The steps involved in performing post stack inversion for band limited and sparse layer reflectivity inversions are described below.

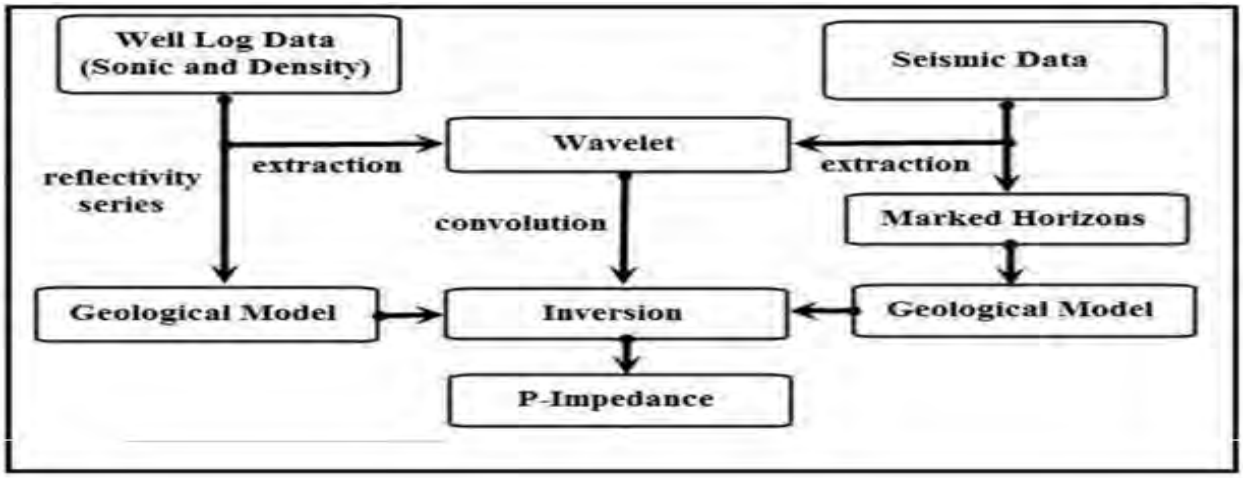

Figure 5.3: Generalized workflow for post stack inversion.

5.3.1 Wavelet extraction and well to seismic tie

Synthetic trace, S(t) is obtained by convolving wavelet with reflectivity series given in equation (5.8) (Barclay et al., 2008), such as:

$$S(t) = W(t) * R + N \tag{5.8}$$

Where W (t) extracted statistical wavelet, (R) reflection coefficient series and N is the random noise. A constant phase wavelet, shown in Figure.5.4, is used to perform correlation between seismic traces close to well location and the synthetic trace obtained from well data by taking the product of sonic and density logs at well DULJAN RE-ENTRY-01. Wavelet is extracted from 2160ms to 2365ms time window, with a wavelength of 200ms. The wavelet extracted is zero phase to obtain reliable results. Wavelet phase shift greatly affects inversion results. If phase shift is higher the error in the impedance results is higher and vice versa (Jain, 2013).

The inversion was performed in zone of interest between 2160 to 2365ms time window. Synthetic seismogram is generated by convolving wavelet (derived from seismic data) with reflectivity series. Then finally, synthetic seismogram is correlated with seismic data for seismic to well tie shown below in Figure 5.5:

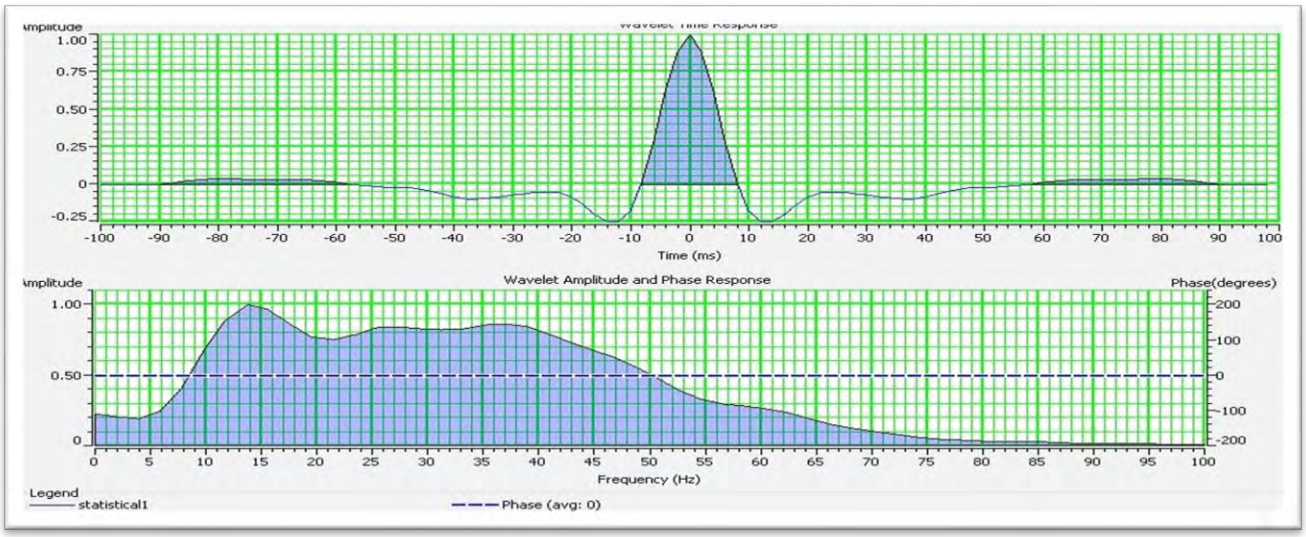

Figure 5.4: Extracted wavelet

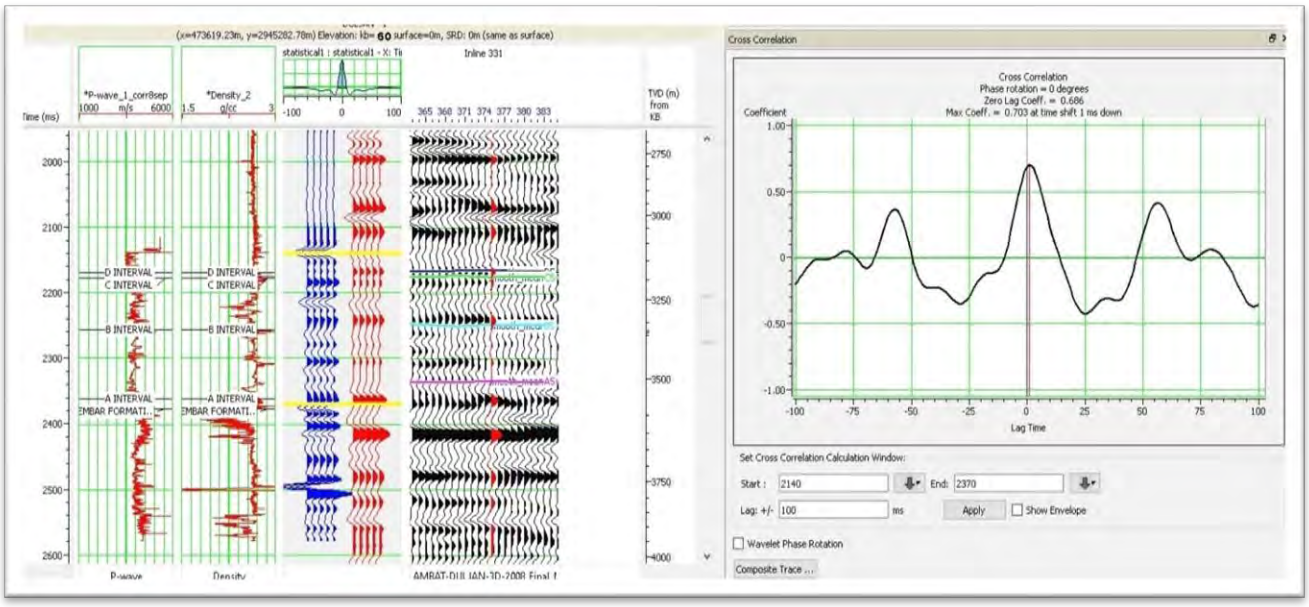

Figure 5.5: Seismic to well tie of DULJAN RE-ENTRY-01 well

5.3.2 Low frequency model

Absolute acoustic impedance gives both qualitative and quantitative results. In absolute acoustic impedance low-frequency model is generated first which is then combined with in inversion algorithms (Cooke and Cant, 2010). Low frequency models are generated from well data to obtain more reliable results (Lindseth, 1979). A low-frequency model generated for band limited and sparse layer reflectivity inversion is shown below in Fig.5.6.

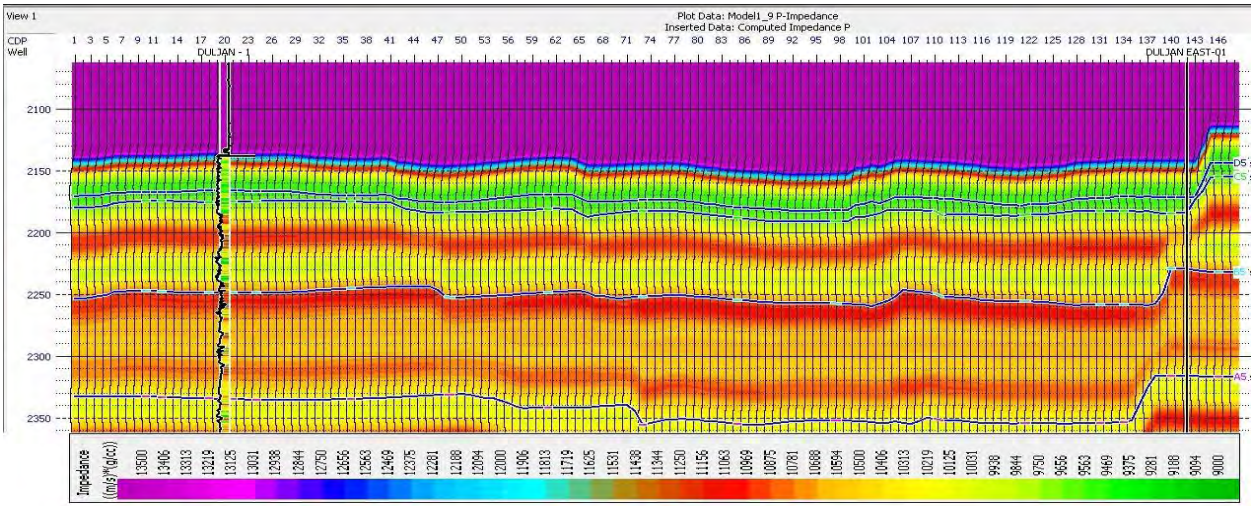

Figure 5.6:Low frequency model used for inversion

5.3.3 Inversion analysis

Inversion analysis window shows the results of seismic to well tie and their correlation is different for different types of inversion. In inversion analysis three windows can been seen, first with filtered impedance log in blue, initial model in black and impedance log in red. The second window shows synthetic trace in red with their correlation with seismic trace(black), correlation value is shown above the window in value form. Third shows root mean square error between both traces.

Results of inversion analysis for Sparse layer reflectivity and band limited post stack inversion are shown in Figures 5.7 and 5.8 below.

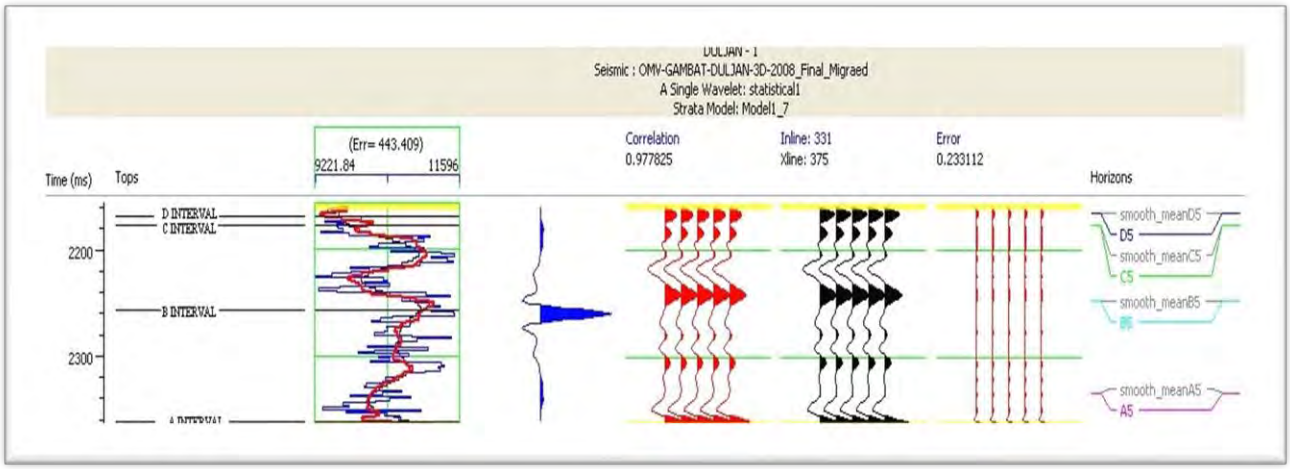

Figure 5.7: Sparse layer reflectivity inversion analysis

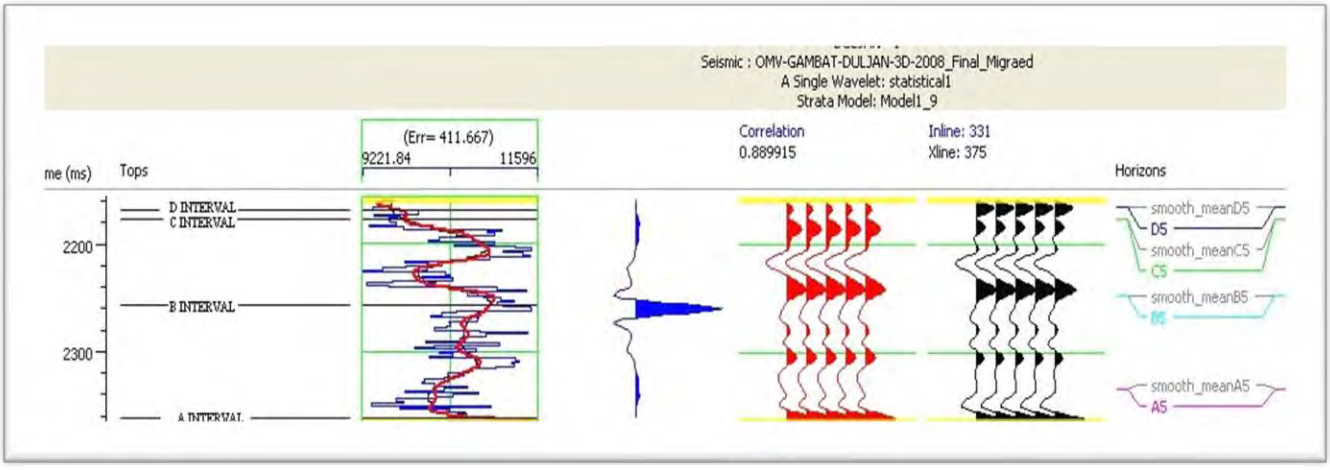

Figure 5.8: Band limited inversion analysis

5.3.4 Results of Sparse layer reflectivity inversion

The correlation between synthetic and seismic traces for DULJAN RE-ENTRY-01 well in sparse layer reflectivity inversion gives correlation of 0.97% and an error of 0.23 or 443 (m/s) (g/cc). The possible zone of interest, two thin gas sand layers marked in figure 5.9 lies in C sand interval between time range of 2120-2240 ms, showing low impedance also confirmed through petrophysical results. This low impedance (9000–10031 (m/s) (g/cc)) shows gas-saturated sands. Furthermore, the high acoustic impedance contrast (between red and green) in Fig.5.9 also shows that this zone is gas saturated. The alternative pattern of medium and high impedances (green, yellow, and red) shown below in figure 5.9 is due to sand-shale layers in the intervals of Lower Goru.

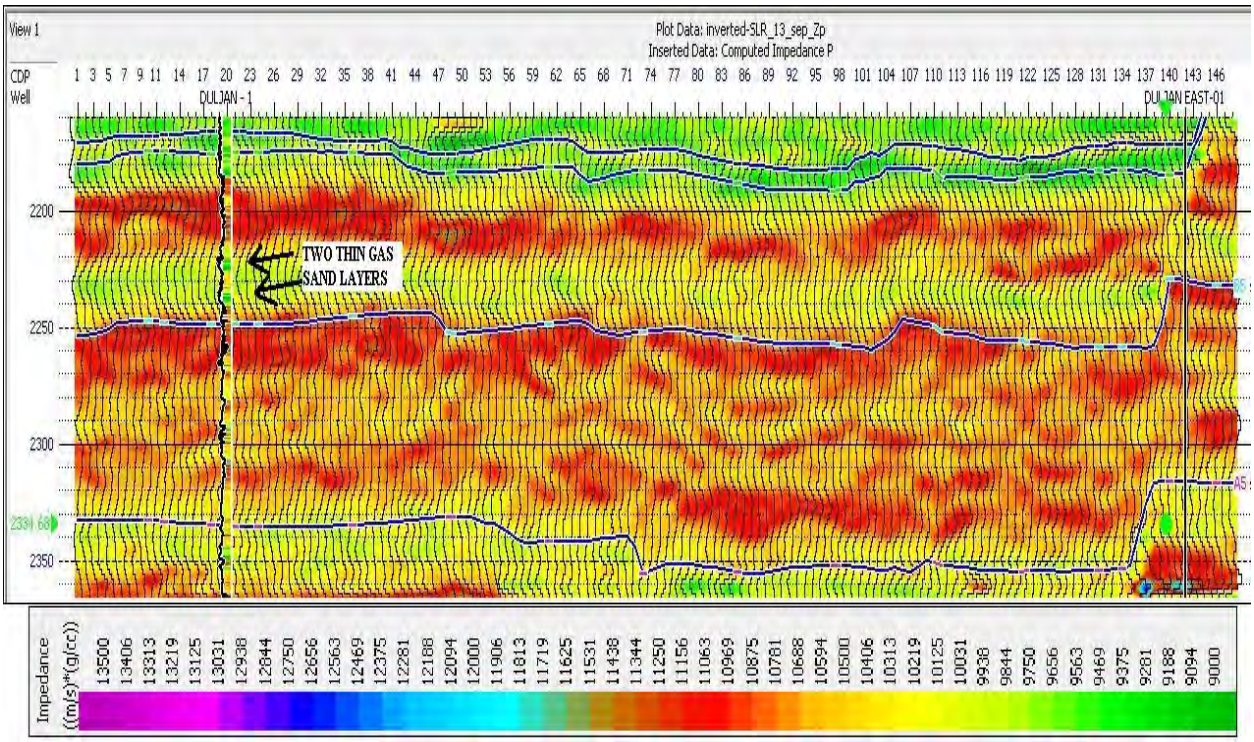

Figure 5.9: Sparse layer reflectivity inversion inverted section

In the above figure, the results of sparse layer reflectivity inversion are shown for interpreted inline 375. The sparse layer reflectivity inversion technique is successfully capturing thin layers of gas

sands imbedded in shales with improved delineation of lateral and vertical variations in acoustic impedances by combining a low-frequency model with good lateral continuity (Fig. 5.6).

5.3.5 Results of Band limited inversion

The correlation between synthetic and seismic traces for DULJAN RE-ENTRY-01 well in band limited inversion gives correlation of 0.88% and an error of 411 (m/s) (g/cc). The results of band limited inversion are shown in figure.5.10 for interpreted inline 375.The band limited inversion technique is successfully capturing thin layers of gas sands imbedded in shales with improved delineation of lateral and vertical variations in acoustic impedances by combining a low-frequency model with good lateral continuity (Fig. 5.6). The possible zone of interest, two thin gas sand layers marked in figure 5.10 lies in C sand interval between time range of 2120-2240ms, showing low impedance also confirmed through petrophysical results. This low impedance (9000–10031 (m/s) (g/cc)) shows gas-saturated sands.

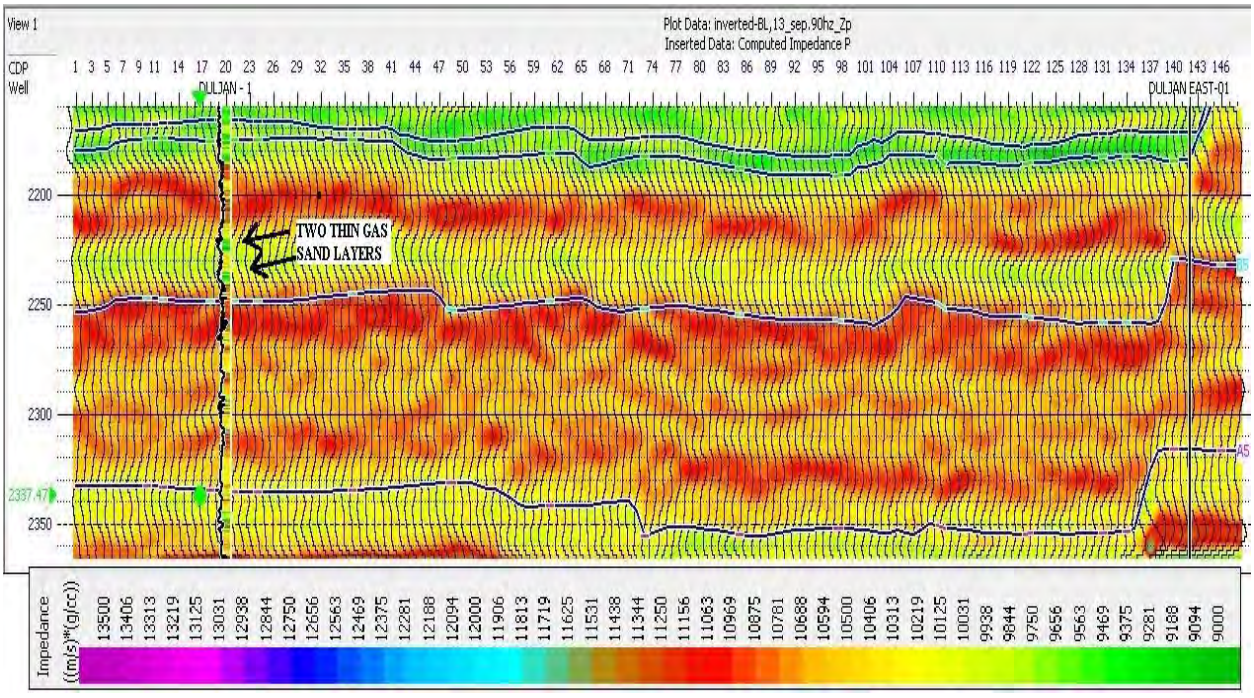

Figure 5.10: Band limited inversion inverted section

Furthermore, the high acoustic impedance contrast (between red and green) in the above figure also shows that this zone is gas saturated. The alternative pattern of medium and high impedances. (green, yellow, and red) shown below in Figure 5.10 is due to sand-shale layers in the intervals of Lower Goru.

5.3.5.1 Impedance and porosity time Slices of Band limited and Sparse layer reflectivity inversion at 2236ms

Impedance and porosity slices of Band limited and Sparse layer reflectivity inversion at 2236ms time are shown below in Figure 5.11 and 5.12.

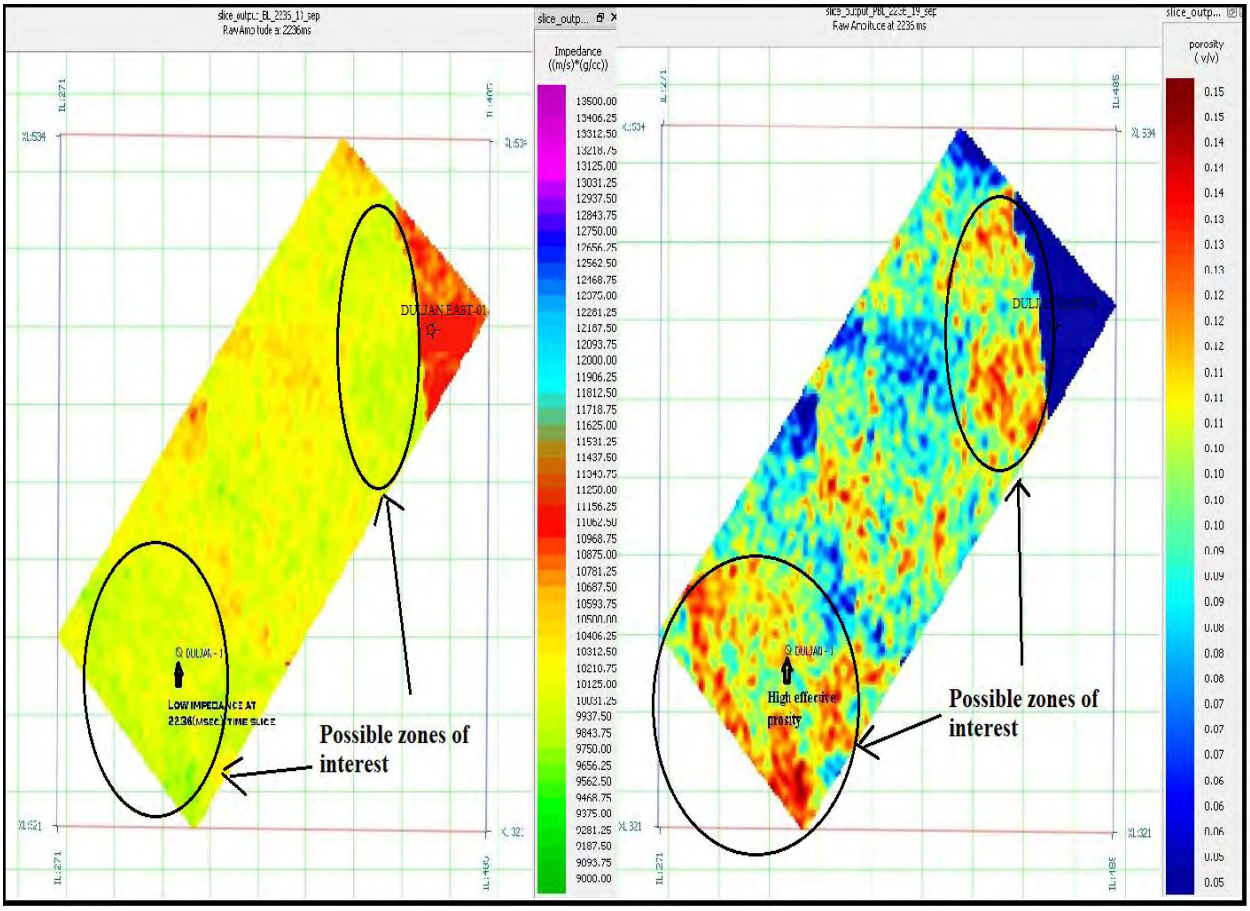

Figure 5.11: Low Impedance and high porosity time slice of Band limited inversion at 2236ms at DULJAN RE-ENTRY-01 well

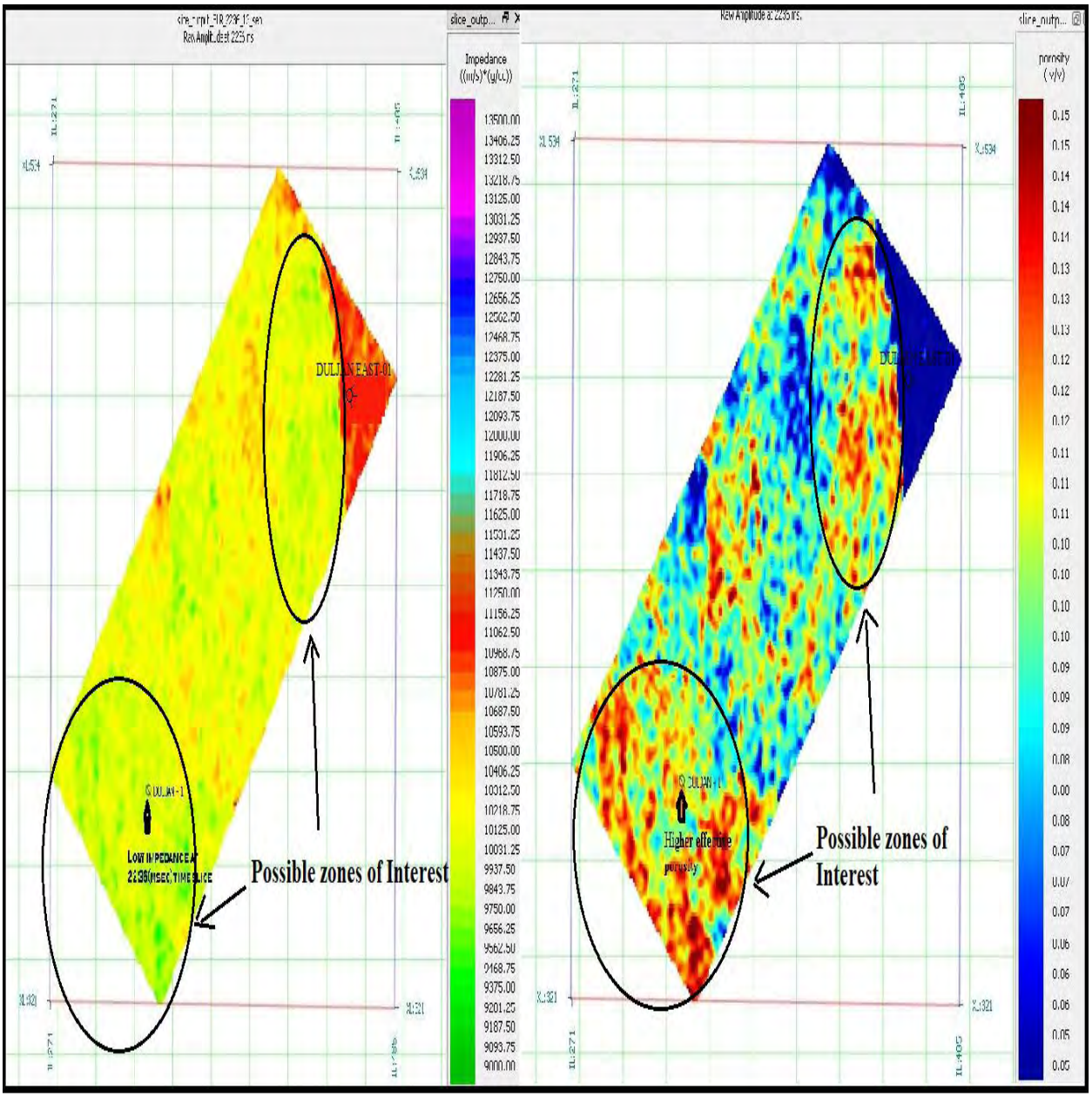

Figure 5.12: Low Impedance and high porosity time Slice of Sparse Layer Reflectivity inversion at 2236ms at DULJAN RE-ENTRY-01 well

Time slices of porosity and impedance slices at 2236ms for Band limited and Sparse Layer Reflectivity inversion shows low impedance (9700(m/s) *(g/cc)) and high effective porosity (0.11 v/v) value at DULJAN RE-ENTRY-01 well location which is zone of interest also confirmed through petrophysical and facies analysis.

5.4 Comparison of results of sparse layer reflectivity and band limited inversion

Two post stack inversion techniques, sparse layer reflectivity and band limited inversion are applied to intervals of lower Goru reservoir formation of DULJAN block and relative performance of each technique has been investigated. Both inversion techniques resolved thin sand shale layering pretty good than the other inversion techniques, but sparse layer reflectivity give better results than band limited inversion in delineating thin sand shale layering. Comparison of both inversions are shown below in table 5.1.

Table 5.1: Comparison of sparse layer reflectivity and band limited inversion results

Inversion type	**Correlation (%)**	**RMS error(m/s) (g/cc)**	**Impedance range (m/s)*(g/cc)**
Sparse layer reflectivity	0.97	443 or 0.23	9221-11596
Band limited	0.88	411	9221-11596

Discussion and Conclusions

Structural interpretation, petrophysical analysis, facies analysis and post stack inversion all play vital roles in improved reservoir characterization of conventional reservoir of Lower Goru Formation. Structural interpretation technique uses seismic and well data to predict the structural style present in the study area and to check whether these structural styles are supporting hydrocarbon accumulation or not. Normal faults is seen in the study area.

In petrophysical analysis well data is used to predict reservoir rock in the area by examining composite log response and petrophysical parameters estimated from these logs. Facies analysis is done to know about the major lithologies present in the area with the help of cross plots of NPHI, RHOB and GR logs. Facies analysis of the study area shows four lithologies present in the area, gas sands (reservoir), shales, sandy shales, and shaly sands. Inversion is performed to delineate the subsurface geology and know the lateral extent of reservoir in the area and to confirm zones of interest(reservoir) marked through petrophysics and facies analysis. Zones of interests show low impedance values and good lateral continuity. In zones of interest(reservoir) acoustic impedance is low (9700 (m/s) *(g/cc)) and effective porosity values are high (0.11 v/v), which confirms it as an effective reservoir. Different Inversion techniques fit for different geological conditions. Comparing Band limited and Sparse Layer reflectivity inversion, Sparse layer reflectivity gives better results than Band limited. Results of all the analysis are supporting each other. The results of these techniques show that C and A intervals are potential reservoir of Lower Goru Formation in DULJAN block.

The conclusions drawn from the study of A, B, C and D intervals of Lower Goru Formation reservoir in DULJAN block are as follows:

The seismic structural interpretation shows the presence of normal faults, having horst and graben structure due to northeast-southwest extensional regime in the study area. Four normal faults are present in the study area.

Petrophysical results show that in C and A intervals effective porosity is high and low values of volume of shale and water saturation. Petrophysical analysis shows that DULJAN RE-ENTRY-01 well has two zones of interests having averages of effective porosity 10%, water saturation 39% and volume of shale 40%. The petrophysical results of DULJAN EAST-01 well shows that it has four zones of interests present in A interval having average effective porosity of 10%, average water saturation 16% and average volume of shale 33%.

Facies analysis results show that there is thin sand shale layering in the study area with dominant shales. Facies analysis shows that there are four lithologies (sand, shale, shaly sand, sandy shale) present in the intervals of Lower Goru reservoir.

Two types of seismic post stack inversion (Band limited and sparse layer reflectivity) are used for improved reservoir characterization of intervals of lower Goru reservoir. Both inversion types confirmed the presence of two thin gas sand layers present in C interval with low impedance values present in time window between 2220-2240ms at DULJAN RE-ENTRY-01 well location. From petrophysical, facies and seismic post stack inversion analysis it was confirmed that C and A intervals are acting as reservoir in DULJAN block. Both the inversion shows pretty good results than other inversion types for delineation of thin sand shale layering but sparse layer reflectivity inversion shows better results than Band limited inversion with correlation of 0.97 for sparse layer reflectivity inversion and correlation of 0.88 for band limited inversion. Impedance and porosity time slices for Band limited and sparse layer reflectivity inversion also shows low impedance (9700 (m/s) *(g/cc)) and high effective porosity(0.11 v/v) values at 2236ms (zone of interest) at DULJAN RE ENTRY-01 well location.

References

Ali, A., Kashif, M., Hussain, M., Siddique, J., Aslam, I., Ahmed, Z., 2015. An integrated analysis of petrophysics, cross-plots and Gassmann fluid substitution for characterization of Fimkassar area, Pakistan: A case study. Arab. J. Sci. Eng. 40, 181–93.

Ahmad, N.; Khan, S.; Al-Shuhail, A. Seismic Data Interpretation and Petrophysical Analysis of Kabirwala Area Tola (01) Well, Central Indus Basin, Pakistan. Appl. Sci. 2021, 11, 2911. [CrossRef]

Ahmad, P. Fink, S. Sturrock, T. Mahmood, M. Ibrahim, Sequence Stratigraphy as Predictive Tool in Lower Goru Fairway, Lower and Middle Indus Platform, Pakistan, PAPG Annual Technical Conference, PAPG, Islamabad, Pakistan, 2004, pp. 85–105.

Atlas D (1979) Log interpretation charts: Dresser Industries. nc., p 107

Archie GE (1942) The electrical resistivity log as an aid in determining some reservoir characteristics. Trans AIME 146:54–62

Ashraf, P. Zhu, Q. Yasin, A. Anees, M. Imraz, H.N. Mangi, S. Shakeel, Classification of reservoir facies using well log and 3D seismic attributes for prospect evaluation and field development: a case study of Sawan gas field, Pakistan, J. Petrol. Sci. Eng. 175 (2019) 338–351.

Ashraf, H. Zhang, A. Anees, M. Ali, X. Zhang, S. Shakeel Abbasi, H. Nasir Mangi, Controls on reservoir heterogeneity of a shallow-marine reservoir in sawan gas field, SE Pakistan: implications for reservoir quality prediction using acoustic impedance inversion, Water 12 (11) (2020) 2972.

Ahmed, H., Cheema, M.R., Fatima, A.N., Iqbal, M.W.A., Raza, H.A., Raza, S. & Ibrahim-Shah, S.M. 1977. Stratigraphy of Pakistan. Memoir, Geological Survey, Pakistan, 12.

Asquith, G. and Krygowski, D. (2004) Basic Well Log Analysis. AAPG Methods in Exploration Series, No. 16, 2004.

Azeem, W.Y. Chun, P. Khalid, L.X. Qing, M.I. Ehsan, M.J. Munawar, X.J. J.o.G. Wei, Engineering, an integrated petrophysical and rock physics analysis to improve reservoir characterization of Cretaceous sand intervals in Middle Indus Basin, Pakistan at 14 (2) (2017) 212–225.

Azeem, W. Yanchun, P. Khalid, L. Xueqing, F. Yuan, C. Lifang, An application of seismic attributes analysis for mapping of gas bearing sand zones in the sawan gas field, Pakistani at 51 (4) (2016) 723–744.

B. Russell, "Machine learning and geophysical inversion — A numerical study," The Leading Edge, vol. 38, no. 7, pp. 512–519, 2019.

Barclay, F., Bruun, A., Rasmussen, K.B., Alfaro, J.C., Cooke, A., Cooke, D., Salter, D., Godfrey, R., Lowden, D., McHugo, S., 2008. Özdemir H. Seismic inversion: reading between the lines. Oilfield Rev. 20 (1), 42–63

Berkhout, "Least-squares inverse filtering and wavelet deconvolution," Geophysics, vol. 42, no. 7, pp. 1369–1383, 1977.

Berger, S. Gier, P. Krois, Porosity-preserving chlorite cements in shallow-marine volcaniclastic sandstones: evidence from Cretaceous sandstones of the Sawan gas field, Pakistan, AAPG Bull. 93 (5) (2009) 595–615.

Blanford, W. T., 1879. The geology of Western Sind. Geol. Surv. India, Mem. 17(1): 1-210.

Blanford, W. T., 1876. On the geology of Sind. Geol. Surv. India, Rec. 9(1): 8-22.

Cooke, D., Cant, J., 2010. Model-based seismic inversion: comparing deterministic and probabilistic approaches. CSEG Rec. 35 (4), 28–39.

Chan, S.A.; Edigbue, P.; Khan, S.; Ashadi, A.L.; Al-Shuhail, A.A. Viscoelastic Model and Synthetic Seismic Data of Eastern Rub'Al-Khali. Appl. Sci. 2021, 11, 1401. [CrossRef]

Castagna, J.P., Batzle, M.L., Kan, T.K., 1993. Rock Physics—The Link between Rock Properties and AVO Response Offset-dependent Reflectivity–Theory and Practice of AVO Analysis, vol. 8. Society of Exploration Geophysicists), Tulsa, OK, pp. 135–171.

Dolan P (1990) Pakistan: a history of petroleum exploration and future potential. Geolog Soc Lond Spec Publ 50:503–524

Dobrin and Savit.,1988, Geophysical Exploration, Hafner Publishing Co.

Debeye and P. Van Riel, "`p-norm deconvolution," Geophysical Prospecting, vol. 38, no. 4, pp. 381–403, 1990.

Eames, F.E. 1952. A contribution to the study of the Eocene in western Pakistan and western India; Part A. The geology of standard sections in the western Punjab and in the Kohat District. Geological Society of London, Quarterly Journal, 107(2): 159–171.

Ehsan, Gu, Z. Ahmad, M.M. Akhtar, S.S. Abbasi, A modified approach for volumetric evaluation of shaly sand formations from conventional well logs: a case study from the talhar shale, Pakistan, Arabian J. Sci. Eng. 44 (1) (2019) 417–428.

Hemphill, W.R. & Kidwai, A.H. 1973. Stratigraphy of the Bannu and Dera Ismail Khan areas, Pakistan. United States Geological Survey, Professional Paper, 716-B: 1–36.

Islam A, Habib M, Islam M, Mita M (2013) Interpretation of wireline log data for reservoir characterization of the Rashidpur Gas Field, Bengal Basin. Bangladesh 1:47–54

Jain, C., 2013. Effect of seismic wavelet phase on post stack inversion. 10th Biennial Int. Conf. exp. P-410. Kadri, I.B., 1995. Pet. Geol. Pak, PPL.

Kemal, A., Balkwill, H.R. & Stoakes, F.A. 1992. Indus basin hydrocarbon plays. In: Ahmad, G.,

Kemal, A., Zaman, A.S.H. & Humayon, M. (Eds), New Directions and strategies for accelerating petroleum exploration and production in Pakistan. Oil and Gas Development Corporation, Islamabad, 78–105.

Krebs, J.R., Anderson, J.E., Hinkley, D., Neelamani, R., Lee, S., Baumstein, A., Lacasse, M.D., 2009. Fast full-wave field seismic inversion using encoded sources. Geophys 74 (6), WCC177–WCC188 DOI.org/10.1190/1.3230502.

Kazmi, A. H., Jan, M. Q. (1997). Geology and tectonics of Pakistan. Karachi, Pakistan. Graphic Publishers, 120 pages.

Khan, A.M.; Al-Juhani, S.G.; Abdul, S. Digital Viscoelastic Seismic Models and Data Sets Of Central Saudi Arabia in the Presence of Near-Surface Karst Features. J. Seism. Explor. 2020, 29, 15–28.

Krois, T. Mahmood, G. Milan, Miano Field, Pakistan, A Case History of Model Driven Exploration, Proceedings Pakistan petroleum convention, 1998, pp. 112–131.

Kadri, I. B. (1995). Petroleum geology of Pakistan. Pakistan Petroleum Ltd, Karachi, Pakistan, 275 pages

Lindseth, R.O., 1979. Synthetic sonic logs – a process for stratigraphic interpretation. Geophysics 44, 3–26 DOI.org/10.1190/1.1440922.

Lindseth R O 1979 Synthetic sonic logs – a process for stratigraphic interpretation; Geophysics 44(1) 3–26.

Mallick, S., 1995. Model-based inversion of amplitude-variations-with-offset data using a genetic algorithm. Geophy 60 (4), 939–954 DOI.org/10.1190/1.1443860.

Munir K, Iqbal M A, Farid A and Shabih S M 2011 Mapping the productive sands of Lower Goru Formation by using seismic stratigraphy and rock physical studies in Sawan area, southern Pakistan: a case study J. Petrol. Explor. Prod. Technol. 133–42

Oldenburg, T. Scheuer, and S. Levy, “Recovery of the acoustic impedance from reflection seismograms,” Geophysics, vol. 48, no. 10, pp. 1318–1337, 1983.

Raza, H. A., Ali, S. M., Ahmed, R. (1990). Petroleum geology of Kirthar sub-basin and part of Kutch basin. Pakistan Journal of Hydrocarbon Research, 2 (1), 27-73.

Raza, Ahmed, Hydrocarbon potential of Pakistan, Journal of Canada Pakistan Cooperation 4 (1) (1990) 9–27.

Shuaib, S. M. (1981). Investigation of prospecting areas and horizons of oil and gas in Pakistan. Geol. Bull. Punjab Univ., 16, 37-42.

Shearer, Introduction to Seismology. Cambridge Univ. Press, 2009.

Soleimani, M. Seismic imaging by 3D partial CDS method in complex media. J. Pet. Sci. Eng. 2016, 143, 54–64. [CrossRef]

Sheriff, R. E., 2002, Encyclopedic dictionary of applied geophysics, 4th edition: Society of Exploration Geophysicists, 429 p

Siddiqui, Petroleum Geology, Basin Architecture and Stratigraphy of Pakistan, 2016. [27] K. Munir, M.A. Iqbal, A. Farid, S.M. Shabih, Mapping the productive sands of Lower Goru Formation by using seismic stratigraphy and rock physical studies in Sawan area, southern Pakistan: a case study, J. Pet. Explor. Prod. Technol. 1 (1) (2011) 33–42.

Taylor, S. C. Banks, and J. F. McCoy, "Deconvolution with the `1 norm," Geophysics, vol. 44, no. 1, pp. 39–52, 1979.

Vredenburg, E. W., 1909b. Mollusca of the Ranikot series, introductory note on the stratigraphy of the Ranikot series. Geol. Surv. India, Mem. Palaegnt. Indica, New Ser., 3, 1: 5-19.

Vredenburg, E. W., 1909a. Report on the geology of Sarawan, Jhalawan, Makran and the State of Lasbela. Geol. Surv. India, Rec. 38, 3: 189-215.

Williams, M. D., 1959. Stratigraphy of the Lower Indus Basin, West Pakistan. Proc. 5th World Petroleum Cong., New York, Sec 1, 19: 377-390.

Yuedong Q and Hongwei A 2007 Study of petrophysical parameter sensitivity from well log data Appl. Geophys. 4 282–7

Yilmaz, ¨ Seismic Data Analysis: Processing, Inversion, and Interpretation of Seismic Data. Society of Exploration Geophysicists, 2001.

Websites

•hhtp/bscgeological.blogspot/2012/04/pakistan.il field.html

•hhtp/A geological study of reservoir formations and exploratory well depths statistical analysis in Sindh Province, Southern Lower Indus Basin, Pakistan.